SANDIA REPORT

SAND98-2880
Unlimited Release
Printed January 1999

Stochastic Parameter Development for PORFLOW Simulations of the Hanford AX Tank Farm

Clifford K. Ho, Robert G. Baca, Stephen H. Conrad, Gary A. Smith, Lih-Jenn Shyr, Timothy A. Wheeler

Prepared by
Sandia National Laboratories
Albuquerque, New Mexico 87185 and Livermore, California 94550

Sandia is a multiprogram laboratory operated by Sandia Corporation, a Lockheed Martin Company, for the United States Department of Energy under Contract DE-AC04-94AL85000.

Sandia National Laboratories

Issued by Sandia National Laboratories, operated for the United States Department of Energy by Sandia Corporation.

Available to DOE and DOE contractors from
Office of Scientific and Technical Information
P.O. Box 62
Oak Ridge, TN 37831

Prices available from (615) 576-8401, FTS 626-8401

Available to the public from
National Technical Information Service
U.S. Department of Commerce
5285 Port Royal Rd
Springfield, VA 22161

NTIS price codes
Printed copy: A04
Microfiche copy: A01

DISCLAIMER

Portions of this document may be illegible in electronic image products. Images are produced from the best available original document.

SAND98-2880
Unlimited Release
Printed January 1999

Stochastic Parameter Development for PORFLOW Simulations of the Hanford AX Tank Farm

Clifford K. Ho[1]
Robert G. Baca[2]
Stephen H. Conrad[3]
Gary A. Smith[4]
Lih-Jenn Shyr[5]
Timothy A. Wheeler[6]

Abstract

Parameters have been identified that can be modeled stochastically using PORFLOW and Latin Hypercube Sampling (LHS). These parameters include hydrologic and transport properties in the vadose and saturated zones, as well as source-term parameters and infiltration rates. A number of resources were used to define the parameter distributions, primarily those provided in the Retrieval Performance Evaluation Report (Jacobs, 1998). A linear rank regression was performed on the vadose-zone hydrologic parameters given in Khaleel and Freeman (1995) to determine if correlations existed between pairs of parameters. No strong correlations were found among the vadose-zone hydrologic parameters, and it was recommended that these parameters be sampled independently until future data or analyses reveal a strong correlation or functional relationship between parameters. Other distributions for source-term parameters, infiltration rates, and saturated-zone parameters that are required to stochastically analyze the performance of the AX Tank Farm using LHS/PORFLOW were adapted from distributions and values reported in Jacobs (1998) and other literature sources. Discussions pertaining to the geologic conceptualization, vadose-zone modeling, and saturated-zone modeling of the AX Tank Farm are also presented.

---

[1] Geohydrology Dept., Sandia National Laboratories, P.O. Box 5800, Albuquerque, NM 87185-0735, ckho@sandia.gov, (505) 844-2384
[2] YMP System Performance Assessments Dept., Sandia National Laboratories, P.O. Box 5800, Albuquerque, NM 87185-0778
[3] Environmental Risk and Decision Analysis Dept., Sandia National Laboratories, P.O. Box 5800, Albuquerque, NM 87185-1345
[4] Dept. of Earth and Planetary Sciences, University of New Mexico, Albuquerque, NM 87131
[5] Transportation Safety and Security Analysis Dept., Sandia National Laboratories, P.O. Box 5800, Albuquerque, NM 87185-0748
[6] Risk Assessment and Systems Modeling Dept., Sandia National Laboratories, P.O. Box 5800, Albuquerque, NM 87185-0747

ACKNOWLEDGMENTS

The authors acknowledge Larry Bustard, Peter Davies, Phil Rogers, Raz Khaleel, and Aki Runchal for their thoughtful reviews, comments, and insightful discussions of this report. This work was performed for the Hanford Tank Initiative Project, in support of the Tank Waste Remediation System, managed by Lockheed Martin Hanford Corporation, Richland, Washington, for the United States Department of Energy, Richland Operations Office, under subcontract number 80232764-9-K001.

CONTENTS

1. INTRODUCTION

In FY97, the United States Department of Energy (DOE) Tank Focus Area (TFA) funded Sandia National Laboratories (SNL) in Albuquerque, New Mexico, to provide technical support to the TFA and various DOE high level waste (HLW) tank sites in addressing critical issues in the areas of HLW tank retrieval and closure. The Hanford Tank Initiative (HTI) desired improved understanding regarding how risks and their uncertainties could be used for comparing tank closure alternatives. SNL was chosen to provide support in these activities because of its background and experience in nuclear power probabilistic risk assessment and radioactive-waste-repository performance assessments (Waste Isolation Pilot Plant and Yucca Mountain).

The Hanford Tank Initiative (HTI) funded Sandia National Laboratories (SNL) in FY98 to conduct uncertainty analyses to support Jacobs Engineering Group's (JEG) Retrieval Performance Evaluation (RPE) Criteria Assessment Project. The objective of the RPE project was to evaluate the potential impact of radionuclide contamination to the groundwater and the public due to releases from a high-level-waste tank farm (AX) at Hanford. The multiphase flow and transport numerical code, PORFLOW (ACRI Inc., 1997), was used in the RPE calculations. While uncertainty analyses were performed using another numerical simulator, MEPAS (Jacobs, 1998), simulations performed with the more rigorous PORFLOW code were performed deterministically. The goal of SNL's task was to implement Sandia's Latin Hypercube Sampling (LHS) software (Wyss and Jorgensen, 1998) into PORFLOW to perform uncertainty analysis in the vadose-zone and groundwater transport models. The LHS program generates multivariate samples of statistical distributions and can implement either Latin hypercube sampling or pure Monte Carlo sampling. Both random and restricted pairing methods can be used to implement multivariate correlations. The union of PORFLOW and LHS allows stochastic simulations to be performed using a state-of-the-art numerical code that simulates multiphase flow and transport processes in the vadose and saturated zones.

Four specific subtasks were identified to best complement the work being performed at JEG: (1) present and document PORFLOW parameter distributions to be used for the uncertainty analysis in a draft report to HTI, (2) implement LHS capability for PORFLOW simulations, (3) assess the feasibility of using high-speed computer platforms at SNL for implementing LHS/PORFLOW uncertainty analysis, and (4) perform LHS/PORFLOW simulations to generate uncertainty for Tc-99 groundwater concentrations at selected receptor locations for one alternative and report the results in a final report to HTI. This draft report identifies the stochastic model parameters and associated distributions that need to be considered in performing the combined LHS/PORFLOW simulations. Issues related to the conceptual model are also documented for further evaluation. This document will serve as the basis for the uncertainty analysis to be continued in FY99.

2. CONCEPTUAL MODEL OF FLOW AND TRANSPORT

The conceptual model of flow and transport at the Hanford AX Tank Farm consists of a contaminant source term, infiltrating water from precipitation, and transport pathways that include the vadose and saturated zones. The exposure to a receptor is not considered in the parameter development in this report. As shown in Figure 1, the contaminant transport originates from a source term, which consists of leaks from the Hanford AX tanks. The leaks are comprised of past leaks (predominantly from the vent headers), retrieval leaks from sluicing operations, and future leaks from residual waste remaining in the tanks. The contaminant is leached by infiltrating water and propagates downward to the water table. The rates and pathways of contaminant transport through the vadose zone are governed, in part, by vadose-zone hydrologic and transport properties. Similarly, saturated-zone hydrologic and transport properties govern the movement of the contaminants in the aquifer until they reach a designated receptor.

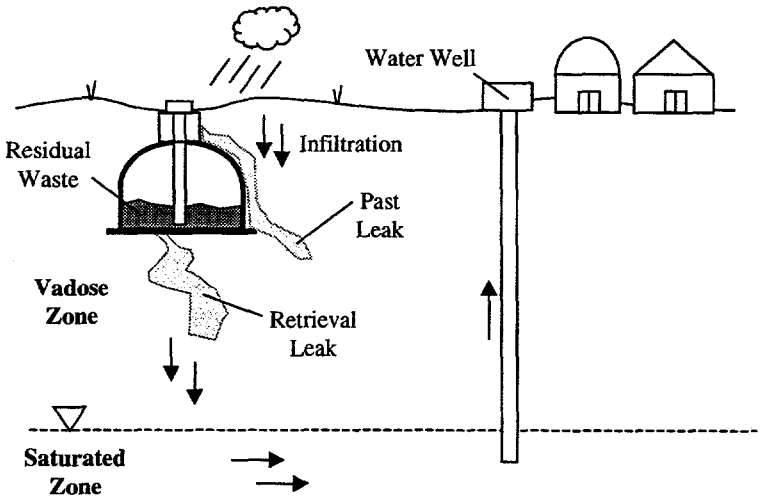

Figure 1. Conceptual sketch of flow and transport at the Hanford AX Tank Farm (adapted from Jacobs, 1998). Not to scale.

Uncertainty and variability exists in the parameters associated with the components of the conceptual model of flow and transport shown in Figure 1. Distributions for these parameters are identified and developed in the following sections in this report for use in the LHS/PORFLOW coupled simulations:

- Source Term

- Infiltration/Recharge
- Vadose-Zone Hydrologic Properties
- Vadose-Zone Transport Properties
- Saturated-Zone Hydrologic Properties
- Saturated-Zone Transport Properties

3. SOURCE TERM

Three sources of radionuclides can contribute to the contamination of the water in the aquifer below the tank farm. The first source is referred to as the "past leak", or the existing contamination of soil near the tank that resulted from the historical leakage of waste from the tank into the soil. The second source is the radioactive waste that would be leaked from the tank into the soil during the use of high-pressure water jets used to dissolve and clean up the waste in the tank. This source is referred to as the "retrieval leak." The third source refers to the radioactive material that may be left in the tank after the tank had been cleaned and prepared for closure. Future releases and leaks resulting from the remaining contaminant is called "residual leaks." In these scenarios, the concentration, solubility, volume, leak duration and timing, and location of the source are uncertain. To incorporate these uncertainties in PORFLOW simulations, distributions of a subset of these parameters have been compiled to describe the three leak scenarios.

3.1. Past Leak

Past leaks have been confirmed to occur near the vent headers of the AX-102 and AX-104 tanks in the 1973 to 1974 timeframe (NHC, 1997). The largest of the past leaks has been postulated to occur from two locations of the vent header attached to the AX-104 tank. The first location is a tee-connector midway between tanks AX-104 and AX-103. The second location is a dresser coupling in the vent header over the tank. In Jacobs (1998), the total leak volume from these two locations near AX-104 was assumed to be equally distributed between the tee-connector and the dresser coupling. In addition, the cumulative contaminant mass from all other past leaks from other tanks in the farm were lumped into these two locations in their model.

The volumetric leak rate in the Jacobs' PORFLOW model was calculated by dividing the leak volume by the assumed duration, which was equal to two years for both leak locations. This flow rate was also modified to account for the volume of the element from which it was being released. In the Jacobs' model, a unit concentration was assumed for the leak, and then the concentrations of individual species were applied in a post-processor to determine the concentration of individual species. Suggested ranges for the leak volume and the concentrations of four radionuclides are presented in Table 1. The ranges and distributions are taken from Table 5.4.3 in the Jacobs (1998) MEPAS uncertainty analysis, but the point estimates are those used in the Jacobs (1998) PORFLOW analysis. The upper and lower bounds for the leak volumes are calculated by using the minimum and maximum reported past leak volumes in Table 5.4.3 in Jacobs (1998), dividing them by the two, and converting the values to m^3. The upper and lower bounds for the concentrations are calculated by calculating the range in Table 5.4.3 in Jacobs (1998) for each species (in appropriate units), and then adding or subtracting half that range to or from the PORFLOW point estimate. If the calculated lower bound using this method was negative (i.e., for C-14, Tc-99, and I-129), the minimum values from Table 5.4.3 in Jacobs (1998) for the past leak concentrations were reported.

Table 1. Suggested distributions for past leak parameters based on PORFLOW point estimates (Jacobs, 1998) and MEPAS uncertainty ranges (Table 5.4.3 in Jacobs, 1998).

Parameter	Point Estimate	Distribution	Lower Bound	Upper Bound
T-Connector Leak Volume (m^3)	15.1	uniform	9.46	37.9
Dresser Coupling Leak Volume (m^3)	15.1	uniform	9.46	37.9
C-14 concentration (Ci/m^3)	2.11E-02	log uniform	3.15E-03	6.67E-02
Se-79 concentration (Ci/m^3)	1.43E-03	log uniform	1.25E-03	1.61E-03
Tc-99 concentration (Ci/m^3)	1.49E-01	log uniform	2.23E-02	4.72E-01
I-129 concentration (Ci/m^3)	2.89E-04	log uniform	4.31E-05	9.13E-04

3.2. Retrieval Leak

In the Jacobs (1998) model, retrieval losses from sluicing were assumed to occur sequentially, beginning with AX-103 in the year 2004 and followed by tanks AX-104, 102, and 101. The duration of the retrieval leaks from the first three tanks were assumed to last 0.5 years, and retrieval losses from AX-101 was assumed to last 1 year for a total duration of 2.5 years. The volumetric leak rate was calculated by dividing the assumed leak volume from each tank by the leak duration. Because the Jacobs (1998) PORFLOW model is two-dimensional, the leaks from tanks AX-101 and 102 were simulated to occur from one of the modeled tanks on the right side of the domain, and leaks from tanks AX-103 and 104 were simulated from the other modeled tank on the left side of the domain. The total volumetric release in the Jacobs (1998) PORFLOW model was scaled by the ratio of the release area in the two-dimensional model to the release area of the three-dimensional tanks. The leaks were assumed to occur over 25% of the actual three-dimensional base of the tank and over 30% of the modeled two-dimensional base of the tank. To ensure equal volumetric flux, the ratio of the areas was used to obtain the modeled flow rate.

Two retrieval leak scenarios were considered in Jacobs (1998): a high retrieval loss and a low retrieval loss. These conditions are used in this report to bound the upper and lower ranges of the retrieval leaks as shown in Table 2. The point estimates of leak volumes for each of the tanks used in Jacobs (1998) for the two scenarios are given by the lower and upper bound values. The lower and upper bounds for the concentrations of four radionuclides are calculated by taking the lower and upper point estimates of the concentrations reported in Jacobs (1998; Table 5.1, Appendix A) for the high and low retrieval loss scenarios. A uniform distribution is assigned to the leak volume and a log uniform distribution is assigned to the concentrations as suggested in Table 5.4.3 in Jacobs (1998).

Table 2. Suggested distributions for retrieval leak parameters based on PORFLOW point estimates (Table 5.1, Appendix A, Jacobs, 1998).

Parameter	Distribution	Lower Bound	Upper Bound
AX-101/102 Leak Volume (m^3)	uniform	30.3	151
AX-103/104 Leak Volume (m^3)	uniform	30.3	151
C-14 concentration (Ci/m^3)	log uniform	6.20E-03	2.89E-02
Se-79 concentration (Ci/m^3)	log uniform	1.13E-03	5.66E-03
Tc-99 concentration (Ci/m^3)	log uniform	7.55E-02	3.62E-01
I-129 concentration (Ci/m^3)	log uniform	8.87E-05	4.14E-04

3.3. Residual Leak

Residual leaks from the tanks are assumed to occur because of degradation of the tanks over time. Water infiltrating through cracks will dissolve and leach residual contaminants from the tank. The residual waste volume following retrieval practices is targeted not to exceed 10 m^3. In the uncertainty analysis performed by Jacobs (1998) using MEPAS, the amount of residual loss was a function of the recharge rate, contaminant solubility, and inventory. In the PORFLOW simulations performed by Jacobs (1998), the amount of residual loss was a function of contaminant solubility and inventory—the amount of water available to leach contaminant away from the base of the tanks was determined by the hydrologic flow behavior simulated in PORFLOW. In the PORFLOW simulations, the residual leak was assumed to begin in the year 2031, ten years after the expected completion of a surface barrier in 2021. The residual leak was assumed to occur along the entire half-base of the modeled tank on either left side (AX-103/104) or the right side (AX-101/102) of the two-dimensional vadose-zone model.

Table 3 provides a range of residual inventory for four radionuclides. The point estimates are taken from the PORFLOW analysis of Jacobs (1998), and the range is taken from the range in products of the residual waste volumes and the residual contaminant concentrations listed in Table 5.4.3 in Jacobs (1998). The values for the mass inventory in Table 3 are scaled by the ratio of the modeled two-dimensional tank base area (11.4 m^2) to two of the actual three-dimensional tank base areas (2 x 410 m^2) to obtain a consistent flux. Only one distribution is given for the inventory of each of the four radionuclides. The distribution can be applied to either the left (AX-103/104) or the right (AX-101/102) modeled tanks.

The distributions of solubilities of four radionuclides are reported in Table 4. The point estimates are taken from Table 6.3 in Appendix A of Jacobs (1998), and the ranges are obtained from the log uniform distributions reported in Table 5.4.3 of Jacobs (1998).

Table 3. Suggested distributions for residual leak inventory parameters based on products of the residual waste volumes and the residual contaminant concentrations listed in Table 5.4.3 in Jacobs (1998).

Parameter	Point Estimate		Distribution	Lower Bound	Upper Bound
	AX-101/AX-102	AX-103/AX-104			
C-14 inventory (Ci)	2.63E-03	3.63E-03	log uniform	7.91E-04	8.15E-02
Se-79 inventory (Ci)	0.0111	0.005	log uniform	1.11E-03	1.15E-01
Tc-99 inventory (Ci)	0.0175	0.0256	log uniform	4.94E-03	8.58E-01
I-129 inventory (Ci)	3.41E-05	4.96E-05	log uniform	7.90E-06	8.14E-04

Table 4. Suggested distributions for contaminant solubilities based on Table 5.4.3 in Jacobs (1998). Point estimates are taken from Table 6.3 in Appendix A of Jacobs (1998).

Parameter	Point Estimate	Distribution	Lower Bound	Upper Bound
C-14 solubility (Ci/m^3)	8.9E-04	log uniform	3.10E-05	3.00E-03
Se-79 solubility (Ci/m^3)	2.68E-03	log uniform	2.68E-03[†]	1.20E+00
Tc-99 solubility (Ci/m^3)	1.55E-02	log uniform	1.26E-02	3.02E-01
I-129 solubility (Ci/m^3)	5.6E-06	log uniform	1.61E-06	4.67E-01

[†]The lower bound calculated from Table 5.4.3 in Jacobs (1998) was greater than the point estimate listed in Table 6.3 in Appendix A of Jacobs (1998), so the point estimate was used as the lower bound.

4. INFILTRATION/RECHARGE

The amount of infiltration (recharge) that percolates through the vadose zone is an important parameter since it can significantly affect the mobilization and rate of transport of contaminants to the saturated zone. Several different periods of infiltration need to be implemented in simulations of the Hanford AX Tank Farm to accommodate pre-tank conditions, current conditions, surface barrier conditions, and post-surface barrier conditions.

Pre-tank infiltration conditions occurred before the construction of the AX Tank Farm in 1963. These conditions represent the amount of infiltration that percolated through the vadose zone to the water table in the absence of the tanks. The pre-tank infiltration is required to establish steady-state conditions in the vadose zone. Shrub-covered surfaces are assumed to have existed with a sand-loam soil before tank construction. Estimated infiltration rates range between 0 to 25.4 mm/year (Rockhold et al., 1995), but to ensure consistency with the Jacobs (1998) PORFLOW analysis, a point estimate of 3 mm/year with no distribution is reported in Table 5 to establish consistent steady-state conditions.

Current conditions consist of a sand and gravel surface with no vegetation or surface barrier. This period ranges from 1963 to when the surface barriers are constructed, anticipated for the year 2020. Historical data have been used to estimate ranges of infiltration that vary between 24 to 66 percent of the annual precipitation (Rockhold et al., 1995). Based on these and other studies, Jacobs (1998) recommended a normal distribution for current infiltration conditions ranging from 35 to 165 mm/year with a mean of 100 mm/year in Table 5.4.6 of their uncertainty analysis (see Table 5). The point estimate used in the PORFLOW analysis was 75 mm/year.

Surface barrier conditions are expected to be constructed in 2020. Two types are identified in Jacobs (1998): (1) a Hanford Barrier consisting of ten alternating layers of soil, gravel, and asphalt with a design life of 1,000 years, and (2) a RCRA-Equivalent Surface Barrier consisting of eight alternating layers of soil, gravel, and asphalt with a design life of 500 years. In the Jacobs (1998) PORFLOW analyses, infiltration rates of 0.5 and 1 mm/year were used for the Hanford and RCRA-Equivalent barriers, respectively. Based on these estimates, a uniform infiltration distribution between 0.5 and 1 mm/year is recommended for surface barrier conditions in Table 5. The duration of the period in which the surface barrier will be functional is uncertain, and the duration can be sampled uniformly between 500 and 1000 years.

After the surface barriers have deteriorated, the infiltration rates are expected to increase. The Jacobs (1998) PORFLOW analysis assumed that the infiltration rates would return to pre-tank conditions. However, the distribution that is recommended in Table 5 is based on a broader range (0.1 to 50 mm/year) presented in Table 5.4.6 in Jacobs (1998).

Table 5. Suggested distributions for infiltration rates based on PORFLOW point estimates and MEPAS uncertainty analyses (Jacobs, 1998).

Period	Distribution	Mean (mm/year)	Standard Deviation	Lower Bound (mm/year)	Upper Bound (mm/year)
Pre-tank (before 1963)	-	3	-	-	-
Current (1963-2020)	normal	100	28	35	165
Surface Barrier (500 to 1000 years after 2020)	uniform	-	-	0.5	1
Post-Surface Barrier	normal	3	10	0.1	50

5. VADOSE-ZONE HYDROLOGIC PROPERTIES

A two-dimensional geologic model of the vadose zone in the vicinity of the AX Tank Farm was presented in Piepho et al. (1996). Figure 2 shows a sketch of the modeled east-west cross-section through the AX Tank Farm, illustrating the presence of nine layers including backfill in the vadose zone. The nine layers were assigned properties in the RPE report by matching particle-size distributions (e.g., gravel, sand, silt & clay) reported in Piepho et al. (1996) to particle-size distributions reported in Khaleel and Freeman (1995), who also produced values for hydrologic properties in the vadose zone. Measured hydrologic properties in Khaleel and Freeman (1995) included saturated conductivity, K_s (cm/s), van Genuchten characteristic parameters, α (1/cm) and n (-), and residual and saturated moisture contents, θ_r (-) and θ_s (-) (see Appendix A: Hydrologic Parameters from Khaleel and Freeman (1995).

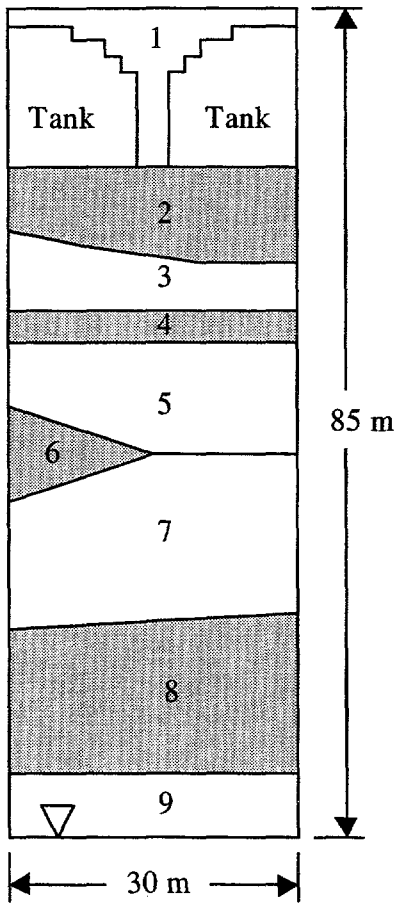

Figure 2. Sketch of the modeled east-west cross section of the vadose zone at the Hanford AX Tank Farm. The nine layers correspond to Piepho et al. (1996). Not to scale.

For their numerical analysis, Jacobs (1998) calculated a bulk-grain-size distribution for a model layer and assigned property values for each layer by comparison to a single sample with a comparable grain-size distribution for which hydraulic properties had been measured (Khaleel and Freeman, 1995). This assumes that the measured hydrologic properties for an individual sample accurately represents the average hydrologic properties of the layer to which it was mapped. While certainly defendable as a first-order approximation, consultation of the vadose-zone hydraulic-property data base (Khaleel and Freeman, 1995) suggests that considerable uncertainty should be attached to the results. Examples are presented below:

1) Layers 3 and 5 (lithostratigraphic unit H2) were assigned a single value, although K_s, for example, ranges over nearly four orders of magnitude within H2 (Khaleel and Freeman, 1995). The value selected for the Jacobs (1998) analysis, 6.63×10^{-3} cm/s, is actually the 75th percentile value from among 53 measurements. The selected value, associated with a sample composed of 10% gravel, 83% sand, and 7% silt and clay, compares well with the presented bulk grain-size distribution of 7% gravel, 87% sand, and 6% silt and clay for layers 3 and 5. The bulk grain-size distribution is, however, arguably more similar to a database sample (borehole 299-E25-234, 33.5 m) composed of 6% gravel, 87% sand, and 7% silt clay, which yields a K_s of 2.82×10^{-4} cm/s. In other words, the method utilized for the Jacobs (1998) analysis could equally well justify selection of K_s values that differ by more than an order of magnitude.

2) The strong layering in the Hanford formation is not represented by selection of a single suite of hydraulic parameters for stratigraphic intervals that are 10-20 m thick. For example, Khaleel and Freeman (1995) present data that indicate order-of-magnitude variation of K_s within H2 over thickness ranges of 5 m or less. The use of a bulk-grain-size distribution averages together coarse and fine-grained layers that are each, on the basis of observations in excavations, generally well sorted. A single suite of hydraulic parameters selected for the bulk sediment does not capture the strong contrasts between alternating low- and high-K_s layers. These contrasts, in turn, produce tension-dependent anisotropy that promotes lateral, rather than vertical, flow. An example of the effect of associated bulk textural properties with a single suite of hydraulic parameters can be seen by comparing the selected values of layers 4, 6, and 8 with those for layers 3, 5 (Jacobs, 1998, Table 5.2.1.). The former assemblage is characterized as being more gravelly yet was assigned a substantially lower K_s value. This unexpected result is partially a result of the selection of hydraulic parameters for units 3 and 5 (see above) but also results from the bulk grain size distribution utilized for units 4, 6 and 8, which consists of 30% gravel, 48% sand, and 22% silt and clay. By comparison to outcrops of Hanford formation, this would be a very unusual grain-size distribution to assign to any one layer, except where soils have developed in loess that has been mixed with sand and gravel by infiltration and bioturbation. The bulk-grain-size distribution averages a strongly layered sequence of interbedded gravel, sand, and silt and, in so doing, does not capture anisotropy, which may dominate vadose-zone flow behavior.

Because of the uncertainty associated with assigning best-estimate hydrologic properties for each unit, we provide hydrologic property distributions (instead of deterministic point values) to be

used in PORFLOW simulations in association with the different layers of the geologic model shown in Figure 1. Table 6 provides a mapping between the layers in the geologic model and the soil categories reported Khaleel and Freeman (1995) based on the particle-size distribution analysis. Additional parameter distributions corresponding to all vadose-zone hydrologic properties reported in Khaleel and Freeman (1995) are also summarized and, where necessary, modified for direct use in LHS.

Table 6. Geologic units reported in Piepho et al. (1996) and corresponding soil categories from Khaleel and Freeman (1995) according to particle size distribution.

Model Layer	Lithology	Particle Size Distribution (%)[2]			Soil Category[3]
		gravel	sand	silt & clay	
1	backfill[1]	-	-	-	-
2	sand and gravel	24	71	5	GS
3, 5	sand and minor gravel	7	87	6	GS
4, 6, 8	sand and gravel	30	48	22	SSG
7	sand	1	90	9	S
9	Ringold Mud	0	78	22	SS

[1] Data used in Jacobs (1998) was taken from Kincaid et al. (1995): $\theta_s = 0.371$, $\theta_r = 0.045$, $\alpha = 0.0683\ cm^{-1}$, $n = 2.08$, and $K_s = 0.03$ cm/s.

[2] From Piepho et al. (1996).

[3] From Khaleel and Freeman (1995): SS = sand mixed with finer fraction, S = sand, SSG = sand and gravel mixed with finer fraction, and GS = gravelly sand.

5.1. Overview of Vadose-Zone Hydrologic Properties

A physical description and overview of the hydrologic properties given in Khaleel and Freeman (1995) are provided in this section. Other parameters used in PORFLOW (e.g., residual saturation, porosity) are also derived from the available hydrologic parameters given in Khaleel and Freeman (1995).

5.1.1. Residual and Saturated Moisture Contents, θ_r and θ_s

The volumetric moisture content, θ, is equal to the ratio of the volume of water in a given volume of porous medium divided by the total volume (rock, liquid, and gas) encompassing that volume of water. As the volume of water in the pores decreases, the residual moisture content, θ_r, is approached. The residual moisture content is defined as the moisture content at which isolated liquid islands are trapped in the interstices of pores and the liquid becomes immobile, even under large pressure gradients. As the volume of water in the pores increases to satiated levels, the saturated moisture content, θ_s, is attained. If we assume that the pores can be completely filled with liquid (no entrapped gas), then the saturated moisture content also provides a measure of the total porosity, ϕ_t:

$$\phi_t = \theta_s \tag{1}$$

In PORFLOW, the residual saturation, S_r, is a required hydrologic parameter for multiphase simulations. The saturation is defined as the volume of fluid divided by the volume of pore space. If the residual gas saturation is assumed to be zero, then the following relation can be used to define the residual liquid saturation, S_r:

$$S_r = \theta_r / \theta_s \tag{2}$$

Finally, the residual and saturated moisture contents can be used to define the effective porosity, ϕ_e. The effective porosity is equal to the volume of pore space that can be satiated by *mobile* liquid divided by the total volume (rock, water, and gas). This quantity can be defined using the residual and saturated moisture contents as follows:

$$\phi_e = \theta_s - \theta_r \tag{3}$$

Equations (1) – (3) can be used to derive parameters required in PORFLOW through the available parameters given in Khaleel and Freeman (1995).

5.1.2. Saturated Conductivity, K_s

The Darcy velocity, v (m/s), (or volumetric flow rate divided by the cross-sectional area of flow) of a fluid through a porous medium can be described by the following equation:

$$v = -K \nabla h \tag{4}$$

where K is the hydraulic conductivity (m/s) and h is the hydraulic head (m). The hydraulic conductivity is a property of the porous medium and can be thought of as a proportionality factor between Darcy velocity and hydraulic gradient. In the vadose zone, the liquid hydraulic conductivity is a strong function of the moisture content. As the liquid saturation increases, the hydraulic conductivity, K, increases until the maximum saturated conductivity, K_s, is attained. This can be illustrated in the following equation for the hydraulic conductivity:

$$K = k\, k_r\, \rho\, g / \mu \tag{5}$$

where k is the intrinsic permeability (m^2), k_r is the fluid relative permeability (-), ρ is the fluid density (kg/m^3), g is the gravitational constant (9.81 m/s^2), and μ is the dynamic viscosity of the fluid (kg/m-s). As the moisture content increases, the liquid relative permeability increases from a minimum value of zero to a maximum value of one under saturated conditions. Therefore, the saturated conductivity, K_s, is given by Equation (5) when the relative permeability is equal to one. During unsaturated conditions, both the relative permeability, k_r, and the hydraulic head, h, must be determined as a function of moisture content, θ. The van Genuchten functions are commonly used to express the conductivity and pressure head as functions of moisture content and are summarized in the following section.

5.1.3. Van Genuchten Parameters, α and n

As introduced in the previous section, equations of flow in unsaturated porous media require relationships that express hydraulic head and relative permeability as functions of moisture content. Van Genuchten (1980) derived empirical functions to describe these relationships, and they can be written as follows:

$$\psi = \frac{1}{\alpha}\left(S_e^{-1/m} - 1\right)^{1-m} \tag{6}$$

$$k_{r,l} = S_e^{0.5}\left(1 - \left(1 - S_e^{1/m}\right)^m\right)^2 \tag{7}$$

where

$$S_e = \frac{\theta - \theta_r}{\theta_s - \theta_r} \tag{8}$$

$$m = 1 - 1/n \tag{9}$$

where ψ (m) is pressure head equal to hydraulic head, h, minus elevation head, z, S_e is an effective saturation (-), α (1/m) and n (-) are van Genucthen fitting parameters, and the subscript l denotes the liquid phase. The van Genuchten α parameter related to the pore size and is inversely proportional to the capillary-rise height (capillary fringe) associated with a porous medium. Larger α values are associated with larger pore sizes and smaller capillary-rise heights due to a decrease in capillary suction potential. The van Genuchten n parameter is associated with the pore-size distribution of a porous medium. Materials that are well graded with similar pore sizes tend to have larger n values. To illustrate the van Genuchten functions, Figure 3 shows plots of the pressure head and relative permeability as a function of moisture content for one soil category (sand) provided in Khaleel and Freeman (1995). Mean property values for sand are used in Equations (6) – (9) and are reported in the plots. As the moisture content decreases from its saturated value, the pressure head (or matric suction potential) increases from a value of zero to extremely large values as the moisture content decreases towards the residual moisture content. Note that the inverse of the van Genuchten α parameter (~9 cm) is approximately equal to the pressure head (also referred to as the air-entry pressure head) required to initiate de-saturation of the sample from its saturated moisture content. In addition, if the van Genuchten n parameter were smaller (larger distribution of pore sizes), the slope of the pressure head curve would become steeper. The liquid relative permeability increases sharply as the moisture content increases, reflecting the increased conductance as larger pores are filled with liquid. The relative permeability curve tends towards sharper inflections as the van Genuchten n parameter becomes smaller. Note also that the van Genuchten α parameter is not used in the relative permeability function.

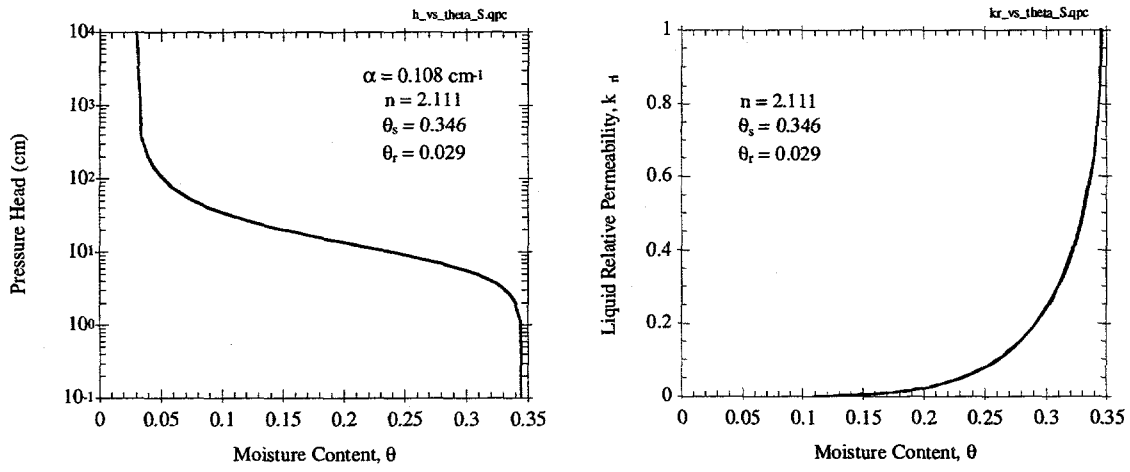

Figure 3. Plots of van Genuchten functions of pressure head and relative permeability as a function of moisture content using mean properties from one soil category (sand) in Khaleel and Freeman (1995).

5.2. Vadose-Zone Property Distributions for LHS

Distributions of the vadose-zone hydrologic properties detailed in the previous section have been compiled by Khaleel and Freeman (1995) for 183 samples taken in the vicinity of the Hanford 200 East and 200 West areas. The purpose of this section is to present these distributions in a manner that is amenable to the LHS software. The LHS software uses the cumulative distribution function of a parameter to create equal probability bins from which to sample. The result is that LHS requires fewer samples than conventional Monte Carlo simulations to obtain accurate estimates of the desired distributions (see Wyss and Jorgensen, 1998).

Several distributions are recognized by the LHS software, including the normal and lognormal distributions reported in Khaleel and Freeman for a number of parameters. Additional parameter distributions (log ratio and hyperbolic arcsine) given in Khaleel and Freeman (1995), but not defined in the LHS software, can still be implemented with several options detailed in this section. The three transformations used in Khaleel and Freeman are expressed below:

lognormal (LN): $$Y = \ln(X) \tag{10}$$

log ratio (LR): $$Y = \ln\left(\frac{X - A}{B - X}\right) \tag{11}$$

hyperbolic arcsin (SN): $$Y = \sin^{-1}(U) = \ln\left(U + (1 + U^2)^{1/2}\right) \tag{12}$$

where $U = (X - A) / (B - A)$

where Y is the transformed variable, X is the untransformed variable, and A and B are the lower and upper limits of the untransformed variable ($A < X < B$).

Table 7 through Table 12 summarize the relevant hydrologic parameter statistics for the six soil categories given in Khaleel and Freeman (1995) for input into LHS. Note that only four soil categories are used in the geologic layers defined by Jacobs (1998) for PORFLOW simulations (see Table 6). For each parameter in each soil category, Khaleel and Freeman (1995) examined the underlying probability distribution using 176 samples. For parameters where the normal distribution was not adequate (as determined by the Kolmogorov-Smirnov goodness of fit test), transformations were used to obtain normal distributions of the parameters. In Table 7 through Table 12, the statistics for the raw data are provided as well as statistics for the transformed parameters.

Table 7. Statistics for hydrologic properties presented in Khaleel and Freeman (1995) for soil category SS (sand mixed with finer fraction).

Parameter	Number of samples	Raw				Transform†	Transformed (normal distribution)			
		Low	High	Mean	Standard Deviation		Upper Limit	Lower Limit	Mean	Standard Deviation
θ_s	48	0.321	0.566	0.438	0.059	NO	-	-	-	-
θ_r	48	0.016	0.110	0.062	0.027	SN	0.000	0.881	0.458	0.255
α (1/cm)	48	8.0e-4	0.387	0.034	0.072	LN	-7.131	-0.949	-4.489	1.352
n	48	1.262	2.894	1.824	0.344	NO	-	-	-	-
K_s (cm/s)	40	5.8e-6	0.017	0.001	0.003	LN	-12.058	-4.057	-8.487	1.813

†NO = Normal (no transformation required); LN = Lognormal; LR = Log ratio; SN = Hyperbolic arcsine

Table 8. Statistics for hydrologic properties presented in Khaleel and Freeman (1995) for soil category S (sand).

Parameter	Number of samples	Raw				Transform†	Transformed (normal distribution)			
		Low	High	Mean	Standard Deviation		Upper Limit	Lower Limit	Mean	Standard Deviation
θ_s	76	0.197	0.519	0.346	0.073	NO	-	-	-	-
θ_r	76	0	0.148	0.029	0.023	SN	0.000	0.881	0.189	0.146
α (1/cm)	76	0.004	0.861	0.108	0.164	LN	-5.547	-0.149	-3.097	1.347
n	76	1.193	4.914	2.111	0.817	LR	-5.756	4.330	-1.459	1.523
K_s (cm/s)	71	1.38e-5	0.058	0.006	0.011	LN	-11.191	-2.847	-6.849	2.129

†NO = Normal (no transformation required); LN = Lognormal; LR = Log ratio; SN = Hyperbolic arcsine

Table 9. Statistics for hydrologic properties presented in Khaleel and Freeman (1995) for soil category SSG (sand and gravel mixed with finer fraction).

Parameter	Number of samples	Raw				Transform†	Transformed (normal distribution)			
		Low	High	Mean	Standard Deviation		Upper Limit	Lower Limit	Mean	Standard Deviation
θ_s	6	0.187	0.375	0.262	0.072	NO	-	-	-	-
θ_r	6	0	0.064	0.030	0.029	NO	-	-	-	-
α (1/cm)	6	0.003	0.103	0.032	0.036	LN	-5.843	-2.276	-3.957	1.166
n	6	1.256	1.629	1.400	0.131	NO	-	-	-	-
K_s (cm/s)	6	2.76e-5	0.068	0.015	0.027	LR	-10.854	2.995	-5.262	5.499

†NO = Normal (no transformation required); LN = Lognormal; LR = Log ratio; SN = Hyperbolic arcsine

Table 10. Statistics for hydrologic properties presented in Khaleel and Freeman (1995) for soil category GS (gravelly sand).

Parameter	Number of samples	Raw				Transform†	Transformed (normal distribution)			
		Low	High	Mean	Standard Deviation		Upper Limit	Lower Limit	Mean	Standard Deviation
θ_s	10	0.203	0.334	0.272	0.048	NO	-	-	-	-
θ_r	10	0.010	0.069	0.040	0.019	NO	-	-	-	-
α (1/cm)	10	0.004	0.074	0.027	0.023	NO	-	-	-	-
n	10	1.529	2.537	1.994	0.315	NO	-	-	-	-
K_s (cm/s)	10	5.43e-5	0.008	0.003	0.003	LR	-7.966	2.989	-1.569	3.582

†NO = Normal (no transformation required); LN = Lognormal; LR = Log ratio; SN = Hyperbolic arcsine

Table 11. Statistics for hydrologic properties presented in Khaleel and Freeman (1995) for soil category SG1 (sandy gravel with gravel fraction < 60%).

Parameter	Number of samples	Raw				Transform†	Transformed (normal distribution)			
		Low	High	Mean	Standard Deviation		Upper Limit	Lower Limit	Mean	Standard Deviation
θ_s	25	0.113	0.260	0.166	0.036	NO	-	-	-	-
θ_r	25	0	0.062	0.023	0.015	NO	-	-	-	-
α (1/cm)	25	0.002	0.919	0.083	0.204	LN	-6.075	-0.084	-4.086	1.550
n	25	1.262	2.947	1.660	0.355	LN	0.233	1.081	0.489	0.184
K_s (cm/s)	24	1.9e-7	0.037	0.005	0.009	LN	-15.476	-3.297	-7.932	3.322

†NO = Normal (no transformation required); LN = Lognormal; LR = Log ratio; SN = Hyperbolic arcsine

Table 12. Statistics for hydrologic properties presented in Khaleel and Freeman (1995) for soil category SG2 (sandy gravel with gravel fraction > 60%).

Parameter	Number of samples	Raw				Transform†	Transformed (normal distribution)			
		Low	High	Mean	Standard Deviation		Upper Limit	Lower Limit	Mean	Standard Deviation
θ_s	11	0.056	0.107	0.077	0.016	LN	-2.888	-2.234	-2.590	0.216
θ_r	11	0	0.020	0.010	0.007	NO	-	-	-	-
α (1/cm)	11	0.003	0.028	0.009	0.009	LN	-5.952	-3.590	-5.008	0.882
n	11	1.347	1.885	1.621	0.178	NO	-	-	-	-
K_s (cm/s)	10	2.83e-5	0.13	0.014	0.041	LN	-10.473	-2.040	-7.137	2.332

†NO = Normal (no transformation required); LN = Lognormal; LR = Log ratio; SN = Hyperbolic arcsine

The LHS software recognizes the normal (NO) and lognormal (LN) distributions and can use the summary statistics in Table 7 through Table 12 directly. For example, the LHS input for the normal distribution of the van Genuchten parameter n in soil category SS would be as follows:

```
n_SS  1.824 BOUNDED NORMAL     1.824 0.344 1.262 2.894
```

The above example defines a bounded normal distribution for a parameter, n_SS (this name can be up to 16 characters long), with a prescribed point value estimate of 1.824 (this value is optional). The last four numbers are the mean, standard deviation, lower bound, and upper bound of the normal distribution. The following example is for LHS input for a lognormal distribution of the saturated conductivity parameter K_s in soil category S:

```
Ks_S  0.006  BOUNDED LOGNORMAL-N  -6.849  2.129  1.38e-5  0.058
```

The above example produces a lognormal distribution based on an underlying (transformed) normal distribution with mean = -6.849 and standard deviation equal to 2.129. A point estimate of 0.006 is specified for the mean of the raw data. Sampling is restricted between the lognormal distribution (raw) values of 1.38e-5 and 0.058. Note that units of saturated conductivity are reported in cm/s here and can be converted to units desired by the user after samples are obtained in LHS.

For distributions other than the normal or lognormal distributions, a couple options can be implemented for use in LHS: (1) the underlying normal distribution can be specified in the LHS input for either the log ratio or hyperbolic distributions followed by a post-processed back-transformation or (2) a pre-processor can be used to generate a back-transformed distribution from the underlying normal distributions a priori for direct input in LHS. In both methods, the following back-transformations of Equations (10) – (12) required:

Back-transformations:

log ratio (LR):
$$X = \frac{Be^{Y} + A}{1 + e^{Y}} \tag{13}$$

hyperbolic arcsine (SN):
$$X = A + 0.5\,(B - A)\,(e^{Y} - e^{-Y}) \tag{14}$$

In the first method the underlying normal distribution of either the log ratio or hyperbolic arcsine distribution is entered into LHS. Then, a post-processor (part of the LHS software) must be run using the back-transformation in Equation (14). The back-transformation can be written out explicitly in the LHS input file using the variable names defined for the input parameters. As an example, the log ratio distribution for the van Genuchten n parameter, in soil category S can be input as follows:

```
n_S    2.111  BOUNDED NORMAL  -1.459  1.523  -5.756  4.330
```

In this example, a point value for the mean of the log ratio distribution is optionally specified as 2.111. The mean and standard deviation of the underlying normal distribution are –1.459 and 1.523, respectively, and samples will be taken between the limits of –5.756 and 4.330 from the underlying normal distribution. Once these samples are obtained, Equation (13) must be used to back-transform the samples to the original log ratio distribution.

In the second method, the cumulative distribution functions for the underlying normal distributions of the log ratio and hyperbolic arcsine distributions are first determined using standardized normal curves. The standardized variables, z, are then back-transformed using the standardized back-transform and either Equations (13) or (14). The variables and their cumulative distribution functions must then be printed to an LHS-readable file. A pre-processor has been written to perform these functions (see Appendix B: Code Listing for Implementation of New Parameter Distributions into LHS), and the LHS input using this method for the previous example is given as follows:

```
n_S                0.21110E+01  CONTINUOUS LINEAR  134 #
0.11979E+01    0.00000E+00  # $ Actual CDF=  0.33700E-03
0.11996E+01    0.68718E-03  #
0.12019E+01    0.13500E-02  #
0.12051E+01    0.25552E-02  #
0.12094E+01    0.46612E-02  #
0.12152E+01    0.81975E-02  #
0.12231E+01    0.13903E-01  #
0.12337E+01    0.22750E-01  #
0.12480E+01    0.35930E-01  #
0.12671E+01    0.54799E-01  #
     .              .
     .              .
     .              .
0.46319E+01    0.99534E+00  #
0.46512E+01    0.99598E+00  #
0.46860E+01    0.99702E+00  #
0.47165E+01    0.99781E+00  #
0.47431E+01    0.99841E+00  #
0.47663E+01    0.99886E+00  #
0.47865E+01    0.99918E+00  #
0.48191E+01    0.10000E+01  # $ Actual CDF=  0.99960E+00
```

In the above listing, a continuous linear distribution (a user-defined distribution recognized in LHS) has been prescribed for the van Genuchten n parameter in soil category S. The mean of the raw log ratio distribution has been optionally specified as 2.111. The number of points that were generated by the pre-processor (using adaptive stepping to prevent the change in the untransformed variable from being greater than one percent) is 134. The next 134 lines (only the beginning and end of the list is shown for brevity) contains the back-transformed variable from the original log ratio distribution and the associated cumulative distribution function. The first and last entries must list cumulative distribution functions of 0.0 and 1.0 for LHS, so the actual

cumulative distribution functions are listed in comments (denoted by $). Note that the # symbol denotes continuation on the next line.

Both methods presented to implement log ratio and hyperbolic arcsine distributions use the cumulative distribution functions adapted from the transformed underlying normal distribution. As shown in Khaleel and Freeman (1995), the transformations to produce the underlying normal distributions (where needed) produced accurate representations of the actual data. Of course, the raw data could also be used directly to create cumulative distributions using discrete values, but several soil categories reported in Khaleel and Freeman (1995) contained very sparse data. Figure 4 shows an example of the cumulative distribution function for the van Genuchten *n* parameter comparing raw data to standard normal cumulative distribution functions derived from a log ratio transformation of the parameter. The parameter values shown are untransformed variables.

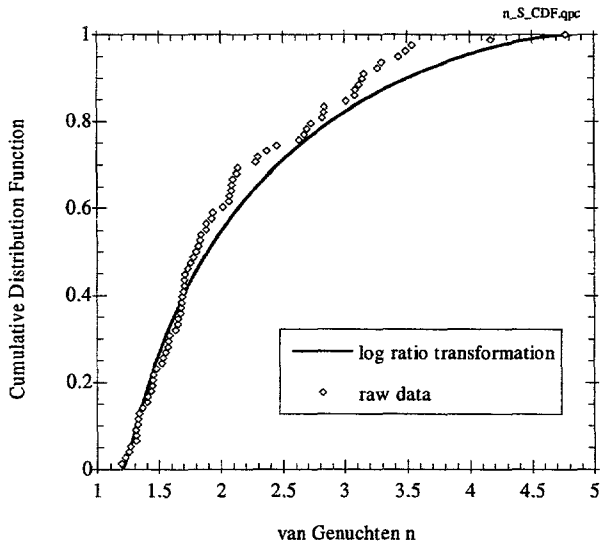

Figure 4. Empirical and fitted cumulative distribution functions of van Genuchten *n* parameter for soil category S in Khaleel and Freeman (1995).

5.3. Assessment of Parameter Correlations

The parameter distributions presented in Section 5.2 can be sampled and paired randomly or with restricted pairing to honor correlations among parameters in LHS. This section provides an assessment of sample correlations using a rank regression between all combinations of parameters given in Khaleel and Freeman (1995). The rank regression is performed on samples belonging to each of the six soil categories described in Khaleel and Freeman (1995) as well as on the entire sample population.

The advantage to performing a rank regression over a regression on the actual parameter values is that a simple linear regression will provide the necessary statistics (i.e., sample correlation coefficient, R) to determine if correlations exist among parameters. A program was written to rank each parameter in a given sample and then perform a regression on the ranked values for different combinations of parameters (see Appendix C: Code Listing for Linear Rank Regression of Hydrologic Parameters). For the five hydrologic parameters reported in Khaleel and Freeman (1995), a total of ten combinations (ordering not important) exists for all parameter pairs. The program was written to conveniently print out a matrix of these parameter combinations with the corresponding sample correlation coefficient for each pair. In addition, the slope and y-intercept are also calculated for a least-squares linear fit through the data. To illustrate this procedure, Figure 5 shows a plot of the ranked values of θ_s (residual moisture content or total porosity) as a function of the ranked values of K_s (saturated conductivity) for all soil categories (183 samples). The lowest value of θ_s was assigned a rank of 1, and the highest value of θ_s was assigned a rank of 183. The values of K_s were ranked in an identical fashion. Then, for each of the 183 samples, the rank of θ_s was plotted against the rank of K_s as shown in Figure 5. If the data falls along a line with a positive slope, a positive correlation exists (large values of θ_s tend to be associated with large values of K_s and vice versa). If the data falls along a line with negative slope, a negative correlation exists.

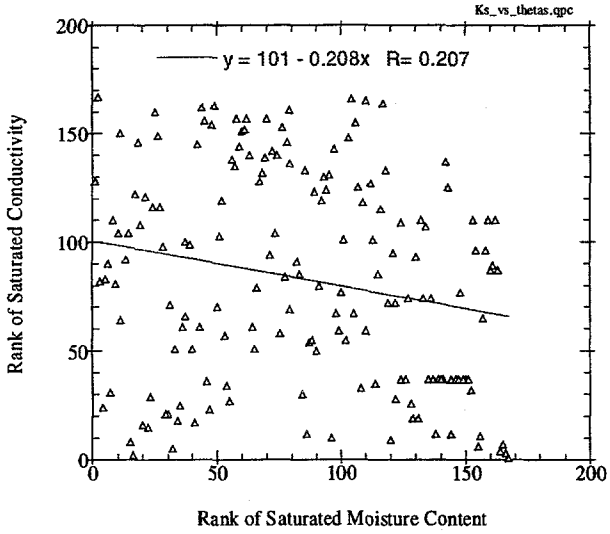

Figure 5. Plot of rank regression of saturated conductivity values as a function of saturated moisture content for all soil categories (167 samples) from Khaleel and Freeman (1995).

Intuitively, one might expect that as the total porosity of a porous medium increases, the saturated conductivity would increase as well, yielding a strong positive correlation coefficient (~ 1). Subsequently, the data should fall close to a straight diagonal line. However, Figure 5 shows that very little correlation exists between these two parameters. Table 13 through Table 15 summarize the statistics (correlation coefficient, R; slope of least-squares linear fit, b_1; and y-intercept of least-squares linear fit, b_0) for the rank regression of five hydrologic parameters for

all soil categories (183 samples) given in Khaleel and Freeman (1995). Note that the matrix of parameter combinations includes pairings of a parameter with itself (yielding R=1), as well as duplicate pairings in transposed cells of the matrix. The sample correlation coefficient, R, the slope of the least-squares linear fit, b_1, and the y-intercept of the least-squares linear fit, b_0, are given in the following expressions (Devore, 1982; pp. 429, 448):

$$R = \frac{N\sum x_i y_i - (\sum x_i)(\sum y_i)}{\sqrt{N\sum x_i^2 - (\sum x_i)^2}\sqrt{N\sum y_i^2 - (\sum y_i)^2}} \tag{15}$$

$$b_1 = \frac{N\sum x_i y_i - (\sum x_i)(\sum y_i)}{N\sum x_i^2 - (\sum x_i)^2} \tag{16}$$

$$b_0 = \frac{\sum y_i - b_1(\sum x_i)}{N} \tag{17}$$

where N is the number of samples and x_i and y_i are the parameter values for sample i. According to Devore (1982; p. 449), a reasonable rule of thumb states that correlation is weak if $0 \leq |R| \leq 0.5$, strong if $0.8 \leq |R| \leq 1.0$, and moderate otherwise. Examination of Table 13 reveals that the correlation is weak between all vadose-zone hydrologic parameters for the entire population of samples given in Khaleel and Freeman (1995). To determine if stronger correlations could be identified if the samples were organized according to the six soil categories identified in Khaleel and Freeman (1995), the correlation coefficient matrix was determined for samples separated into each of the six soil categories (Table 16 through Table 21). In Table 18, moderate to strong correlations are observed for parameters in soil category 3 (sand and gravel mixed with finer fraction), but since only 6 samples comprise this soil category, confidence in this regression is low. In general, results from the additional analyses of individual soil categories do not show evidence of stronger correlations among the parameters.

Table 13. Correlation coefficient matrix for linear rank regression of five hydrologic parameters for all soil categories (183 samples) in Khaleel and Freeman (1995).

correlation coefficient R	van Genuchten α (1/cm)	van Genuchten n	residual moisture content, θ_r	saturated moisture content, θ_s	saturated conductivity, K_s† (cm/s)
α (1/cm)	1.00	-0.23	-0.39	0.03	0.41
n	-0.23	1.00	0.38	0.17	0.20
θ_r	-0.39	0.38	1.00	0.53	-0.19
θ_s	0.03	0.17	0.53	1.00	-0.21
K_s (cm/s)	0.41	0.20	-0.19	-0.21	1.00

†Only 167 samples were used to correlate K_s with other parameters.

Table 14. Slope for linear rank regression of five hydrologic parameters for all soil categories (183 samples) in Khaleel and Freeman (1995).

slope of linear rank regression fit, b_1	van Genuchten α (1/cm)	van Genuchten n	residual moisture content, θ_r	saturated moisture content, θ_s	saturated conductivity, K_s† (cm/s)
α (1/cm)	1.00	-0.23	-0.40	0.03	0.41
n	-0.24	1.00	0.39	0.17	0.20
θ_r	-0.39	0.38	1.00	0.52	-0.19
θ_s	0.03	0.17	0.54	1.00	-0.21
K_s (cm/s)	0.41	0.20	-0.19	-0.20	1.00

†Only 167 samples were used to correlate K_s with other parameters.

Table 15. y-intercept for linear rank regression of five hydrologic parameters for all soil categories (183 samples) in Khaleel and Freeman (1995).

y-intercept of linear rank regression fit, b_0	van Genuchten α (1/cm)	van Genuchten n	residual moisture content, θ_r	saturated moisture content, θ_s	saturated conductivity, K_s† (cm/s)
α (1/cm)	0.00	113.44	127.75	88.82	48.73
n	113.44	0.00	55.40	76.30	66.50
θ_r	127.23	57.61	0.00	44.20	98.78
θ_s	88.65	76.36	41.52	0.00	100.73
K_s (cm/s)	49.88	67.64	99.03	101.01	0.00

†Only 167 samples were used to correlate K_s with other parameters.

Table 16. Correlation coefficient matrix for linear rank regression of five hydrologic parameters for soil category SS (sand mixed with finer fraction: 52 samples) in Khaleel and Freeman (1995).

correlation coefficient R	van Genuchten α (1/cm)	van Genuchten n	residual moisture content, θ_r	saturated moisture content, θ_s	saturated conductivity, K_s† (cm/s)
α (1/cm)	1.00	-0.27	-0.33	0.05	0.56
n	-0.27	1.00	-0.01	-0.45	0.12
θ_r	-0.33	-0.01	1.00	0.42	-0.42
θ_s	0.05	-0.45	0.42	1.00	-0.18
K_s (cm/s)	0.56	0.12	-0.42	-0.18	1.00

†Only 44 samples were used to correlate K_s with other parameters.

Table 17. Correlation coefficient matrix for linear rank regression of five hydrologic parameters for soil category S (sand: 79 samples) in Khaleel and Freeman (1995).

correlation coefficient R	van Genuchten α (1/cm)	van Genuchten n	residual moisture content, θ_r	saturated moisture content, θ_s	saturated conductivity, K_s[†] (cm/s)
α (1/cm)	1.00	-0.53	-0.62	0.04	0.23
n	-0.53	1.00	0.63	0.27	0.24
θ_r	-0.62	0.63	1.00	0.08	0.00
θ_s	0.04	0.27	0.08	1.00	-0.09
K_s (cm/s)	0.23	0.24	0.00	-0.09	1.00

[†]Only 73 samples were used to correlate K_s with other parameters.

Table 18. Correlation coefficient matrix for linear rank regression of five hydrologic parameters for soil category SSG (sand and gravel mixed with finer fraction: 6 samples) in Khaleel and Freeman (1995).

correlation coefficient R	van Genuchten α (1/cm)	van Genuchten n	residual moisture content, θ_r	saturated moisture content, θ_s	saturated conductivity, K_s (cm/s)
α (1/cm)	1.00	-0.37	-0.36	0.09	0.16
n	-0.37	1.00	0.88	0.83	0.67
θ_r	-0.36	0.88	1.00	0.83	0.81
θ_s	0.09	0.83	0.83	1.00	0.93
K_s (cm/s)	0.16	0.67	0.81	0.93	1.00

Table 19. Correlation coefficient matrix for linear rank regression of five hydrologic parameters for soil category GS (gravelly sand: 10 samples) in Khaleel and Freeman (1995).

correlation coefficient R	van Genuchten α (1/cm)	van Genuchten n	residual moisture content, θ_r	saturated moisture content, θ_s	saturated conductivity, K_s (cm/s)
α (1/cm)	1.00	-0.25	-0.71	0.10	0.25
n	-0.25	1.00	-0.02	0.36	0.19
θ_r	-0.71	-0.02	1.00	-0.28	0.15
θ_s	0.10	0.36	-0.28	1.00	0.09
K_s (cm/s)	0.25	0.19	0.15	0.09	1.00

Table 20. Correlation coefficient matrix for linear rank regression of five hydrologic parameters for soil category SG1 (sandy gravel with gravel fraction < 60%: 25 samples) in Khaleel and Freeman (1995).

correlation coefficient R	van Genuchten α (1/cm)	van Genuchten n	residual moisture content, θ_r	saturated moisture content, θ_s	saturated conductivity, K_s† (cm/s)
α (1/cm)	1.00	-0.19	-0.01	0.37	0.45
n	-0.19	1.00	0.38	-0.15	0.13
θ_r	-0.01	0.38	1.00	0.06	-0.06
θ_s	0.37	-0.15	0.06	1.00	0.01
K_s (cm/s)	0.45	0.13	-0.06	0.01	1.00

†Only 24 samples were used to correlate K_s with other parameters.

Table 21. Correlation coefficient matrix for linear rank regression of five hydrologic parameters for soil category SG2 (sandy gravel with gravel fraction > 60%: 11 samples) in Khaleel and Freeman (1995).

correlation coefficient R	van Genuchten α (1/cm)	van Genuchten n	residual moisture content, θ_r	saturated moisture content, θ_s	saturated conductivity, K_s† (cm/s)
α (1/cm)	1.00	0.05	0.05	0.09	-0.62
n	0.05	1.00	0.48	0.21	0.14
θ_r	0.05	0.48	1.00	0.68	0.06
θ_s	0.09	0.21	0.68	1.00	-0.26
K_s (cm/s)	-0.62	0.14	0.06	-0.26	1.00

†Only 10 samples were used to correlate K_s with other parameters.

6. VADOSE-ZONE TRANSPORT PROPERTIES

Properties that affect contaminant transport in the vadose zone include the distribution coefficient, K_d (m^3/kg), effective molecular diffusion coefficient, D_e (m^2/s), effective porosity, ϕ_e (-), longitudinal and transverse dispersivities, α_L and α_T (m), and bulk density, ρ_B (kg/m^3). These parameters can be identified in the following one-dimensional advective-dispersive equation with equilibrium sorption reaction (p. 478, Domenico and Schwartz, 1990):

$$\frac{D_x}{R_f}\frac{\partial^2 C}{\partial x^2} - \frac{v_x}{R_f}\frac{\partial C}{\partial x} = \frac{\partial C}{\partial t} \tag{18}$$

where

$$R_f = 1 + \rho_b K_d / \phi_e \tag{19}$$

$$D_x = D' + D_e \tag{20}$$

$$D'_L = \alpha_L v_x \tag{21}$$

$$D'_T = \alpha_T v_x \tag{22}$$

where C is concentration of the contaminant (kg/m^3), x is the coordinate (m), t is time (s), v_x is the Darcy velocity in the x-direction (m/s) (see Equation (4)), R_f is the retardation factor (-), D_x is the hydrodynamic dispersion coefficient, and D'_L and D'_T are the longitudinal and transverse mechanical dispersion coefficients (m^2/s).

6.1. Vadose-Zone Distribution Coefficients

The distribution coefficient, K_d, is used to describe the reversible, equilibrium partitioning of contaminants between the solid phase and the liquid phase:

$$C_s = K_d C_w \tag{23}$$

where C_s is the concentration on the solid phase (kg/kg) and C_w is the concentration in the liquid water phase (kg/m^3). If the relationship between the solid-phase and liquid-phase concentrations is linear, then the distribution coefficient is defined by the slope. If the value of K_d is large, then sorption onto the solid phase is large and the retardation factor in Equation (19) is large, which reduces the transport quantities of advection and dispersion in Equation (18). The value of the distribution coefficient depends on the solute, waste chemistry, and background chemistry. In general, the near-field (near the tank) exhibits lower solute K_d values because of the existence of higher salt concentrations, which compete for sorption sites on the solid phase. In the Jacobs (1998) PORFLOW analysis, the near field was defined as layers 1–4, which extend to a depth of about 40 m beneath the surface. The far field is assumed for layers 5–9, which extend from ~40

m beneath the surface to the water table at approximately 85 m beneath the surface. Table 22 summarizes values and distributions for K_d values for four radionuclides for both the near and far fields.

Table 22. Distribution coefficients, K_d, for four radionuclides in near-field and far-field regions.

Region		K_d (m^3/kg)				Ref.
		C-14	Se-79	Tc-99	I-129	
Near Field	Point Estimate	0.0	0.0	0.0	0.0	1
	Lower Bound	0.0	0.0	0.0	0.0	2
	Upper Bound	2.0E-04	2.0E-04	2.0E-04	2.0E-04	2
	Distribution	log uniform	log uniform	log uniform	log uniform	3
Far-Field	Point Estimate	6.0E-04	0.0	0.0	6.0E-04	1
	Lower Bound	5.0E-04	0.0	0.0	2.0E-04	4
	Upper Bound	1.0	7.8E-04	6.0E-04	1.5E-02	4
	Distribution	log uniform	log uniform	log uniform	log uniform	3

[1]Jacobs (1998, Section 5.2.1.4.5)
[2]Kincaid et al. (1998, Table E.8, very high salt/very basic)
[3]Engineering judgment
[4]Kincaid et al. (1998, Table E.10, low organic/low salts/near neutral)

6.2. Vadose-Zone Effective Molecular Diffusion Coefficient

The effective molecular diffusion coefficient accounts for free-water molecular diffusion and the effects of the porous medium on the tortuosity and reduced area available for diffusion. As reported in Jacobs (1998), typical free-water molecular diffusion coefficients for major ions range from 0.03 to 0.06 m^2/year. These values can be reduced by two orders of magnitude because of increased tortuosity and reduced diffusive area in a porous medium. Walton (1985) reported typical ranges of the effective molecular diffusion coefficient to be between 3.15×10^{-4} and 3.15×10^{-2} m^2/year. In Jacobs (1998) PORFLOW analysis, a point estimate of 1.46×10^{-3} m^2/year was used for all effective molecular diffusion coefficients. The impact of this parameter on the overall performance of the site is expected to be minimal, so the point estimate is recommended for use in the LHS/PORFLOW stochastic simulations. If a distribution is desired, a uniform distribution between 3.15×10^{-4} and 3.15×10^{-2} m^2/year can be used.

6.3. Vadose-Zone Effective Porosity

The effective porosity, ϕ_e, is equal to the volume of pore space that can be occupied by mobile fluid divided by the total volume. The effective porosity can be expressed as the difference between the saturated and residual moisture contents as shown in Equation (3). Because the saturated and residual moisture contents are variable, the effective porosity is expected to vary between layers defined in the PORFLOW model. As shown in Equation (19), as the effective porosity increases, the retardation factor, R_f, decreases.

6.4. Vadose-Zone Longitudinal and Transverse Dispersivities

The longitudinal and transverse dispersivities describe the amount of spreading of a solute in groundwater due to local variations in velocity about the mean velocity. Pore-scale heterogeneities give rise to local variability in the flow pattern, causing the variations in velocity. This process associated with the dispersivities is advective in nature, unlike the molecular diffusion process associated with the effective diffusion coefficient. Large values of dispersivity will cause more spreading of the solute in the flow, potentially causing additional dilution of the contaminant.

The longitudinal dispersivity is defined parallel to the flow, and transverse dispersivity is defined perpendicular to the flow. In Jacobs (1998), the longitudinal dispersivity was calculated as one percent of the layer thickness (Schramke et al., 1994). The point estimates used in Jacobs (1998) for the PORFLOW model layers are summarized in Table 23. The suggested uniform distributions are based on an arbitrary twenty percent margin of error for the estimated values of the layer thicknesses. For consistency with the Jacobs (1998) analysis, the transverse dispersivity should be calculated to be ten percent of the longitudinal dispersivity (i.e., $\alpha_T = 0.1\ \alpha_L$).

Table 23. Longitudinal dispersivities for the model layers defined in Jacobs (1998) for the PORFLOW analysis. The point estimates are from Table 5.2.2 in Jacobs (1998).

Layer	Longitudinal Dispersivity, α_L (m)			Distribution
	Point Estimate	Lower Bound	Upper Bound	
1	0.162	0.146	0.178	uniform
2	0.052	0.0468	0.0572	uniform
3	0.122	0.101	0.134	uniform
4	0.03	0.027	0.033	uniform
5	0.091	0.0819	0.100	uniform
6	0.061	0.0549	0.0671	uniform
7	0.203	0.183	0.223	uniform
8	0.091	0.0819	0.100	uniform
9	0.031	0.0279	0.0341	uniform

6.5. Vadose-Zone Bulk Density

The bulk density, ρ_b, is required to calculate the retardation factor in Equation (19). The bulk density is equal to the mass of solid divided by the total volume occupied by solid, liquid, and gas. It is a function of the particle density, ρ_p, and the total porosity, ϕ_t, and can be expressed as follows:

$$\rho_b = (1 - \phi_t)\ \rho_p \tag{24}$$

The particle density is assumed to be constant and equal to 2650 kg/m^3 for all layers in the Jacobs (1998) PORFLOW model. Therefore, the variable in the bulk density will result from variations in the total porosity given in Equation (1).

7. SATURATED-ZONE HYDROLOGIC PROPERTIES

The saturated-zone model used in the Jacob's PORFLOW model (1998) is a two-dimensional model describing the horizontal flow and transport in an unconfined aquifer beneath the AX Tank Farm. The model consists of 37,541 nodes (173 x 217) of which 12,894 are in the active portion of the model domain. Each finite volume grid cell is 250 m x 250 m x 1 m. The two-dimensional model is an adaptation of the three-dimensional transient model used in the Composite Analysis described in Kincaid et al. (1998). The boundaries for the two-dimensional model include the Rattlesnake Hills, Yakima Ridge, Umtanum Ridge, and the Columbia and Yakima rivers, which is consistent with the boundaries used in Kincaid et al. (1998). Additional details of the model domain and boundary conditions can be found in Section 5.2.2 in Jacobs (1998).

Because the saturated-zone flow is assumed to be steady, the only hydrologic parameter of interest is the saturated conductivity of the different aquifer units (see Table 5.2.5 in Jacobs, 1998). However, because the model is two-dimensional and assumed to have a unit thickness in the vertical direction, an effective transmissivity, T, is implemented that accounts for horizontal flow in multiple layers. The effective transmissivity is calculated as follows for each of the nodes in the model:

$$T = \Sigma K_i b_i, \; i = 1 \text{ to } N \tag{25}$$

where b is the unit thickness in the vertical direction (m) and N is the number of units in the portion of the aquifer of interest. In the PORFLOW model performed by Jacobs (1998), the 12,894 nodal transmissivity values, which were assumed isotropic, were consolidated to 200 zones of different transmissivities to accommodate limitations in PORFLOW. To develop distributions for the transmissivities used in the LHS/PORFLOW simulations, the 200 zones were partitioned to four "T-bins" (consistent with the four transmissivity zones illustrated in Figure 5.2.16 in Jacobs, 1998) that span the following ranges of transmissivities: 4,000–120,000 m^2/year; 120,00–240,000 m^2/year; 240,000–1,000,000 m^2/year; and 1,000,000–32,000,000 m^2/year (see Table 24). In Table 24 the mean of the transmissivities in each T-bin is provided for use as point estimates in the LHS input file.

Table 24. Transmissivity bins (*T*-bins) and associated ranges, PORFLOW materials, and means for use in LHS.

T-Bin	Transmissivity Range (m^2/year)	PORFLOW Materials	Mean (m^2/year)
1	4,000–120,000	1-64	6.45E+04
2	120,000–240,000	65-114	1.75E+05
3	240,000–1,000,000	66-160	4.45E+05
4	1,000,000–32,000,000	161-200	4.96E+06

In each *T*-bin, the cumulative distribution functions of the transmissivity values are evaluated for input to LHS. The values of each of the 200 transmissivities used in the PORFLOW simulations are used directly. Plots of the cumulative distribution functions for each of the four *T*-bins are shown in Figure 6. The distributions in the first two *T*-Bins appear to be uniform in nature, whereas the distributions in the last two *T*-bins appear to trend towards a log normal distribution. In LHS, a continuous linear distribution can be used to implement the cumulative distribution functions in Figure 6. An example of the LHS input file for *T*-bin 2 is shown below:

```
$T-bins: 1 = 4e3-1.2e5; 2 = 1.2e5-2.4e5; 3 = 2.4e5-1e6; 4 = 1e6-3.2e7
$
T-bin2_65-114      1.75e5  CONTINUOUS LINEAR  51  #
120000       0.00  #
120043.1     0.02  #
122530.4     0.04  #
123480.1     0.06  #
126058.7     0.08  #
127607.4     0.10  #
129616.3     0.12  #
131431.6     0.14  #
    .          .
    .          .
    .          .
215391.6     0.86  #
217195.9     0.88  #
219332.6     0.90  #
223591.4     0.92  #
226601.1     0.94  #
232090.8     0.96  #
237197       0.98  #
238822.4     1.00  #
```

Once the four *T*-bins have been sampled using LHS, then each of the materials listed in Table 24 can be assigned an appropriate sampled value for transmissivity. Two options exist for assigning sampled transmissivities to PORFLOW materials. The first is to sample a new value for each of the 200 materials. The second is to use one sampled value to represent all materials belonging to each of the four *T*-bins. Because of the large number of materials used in the PORFLOW

saturated-zone simulation, we recommend the second option to reduce the number of required realizations.

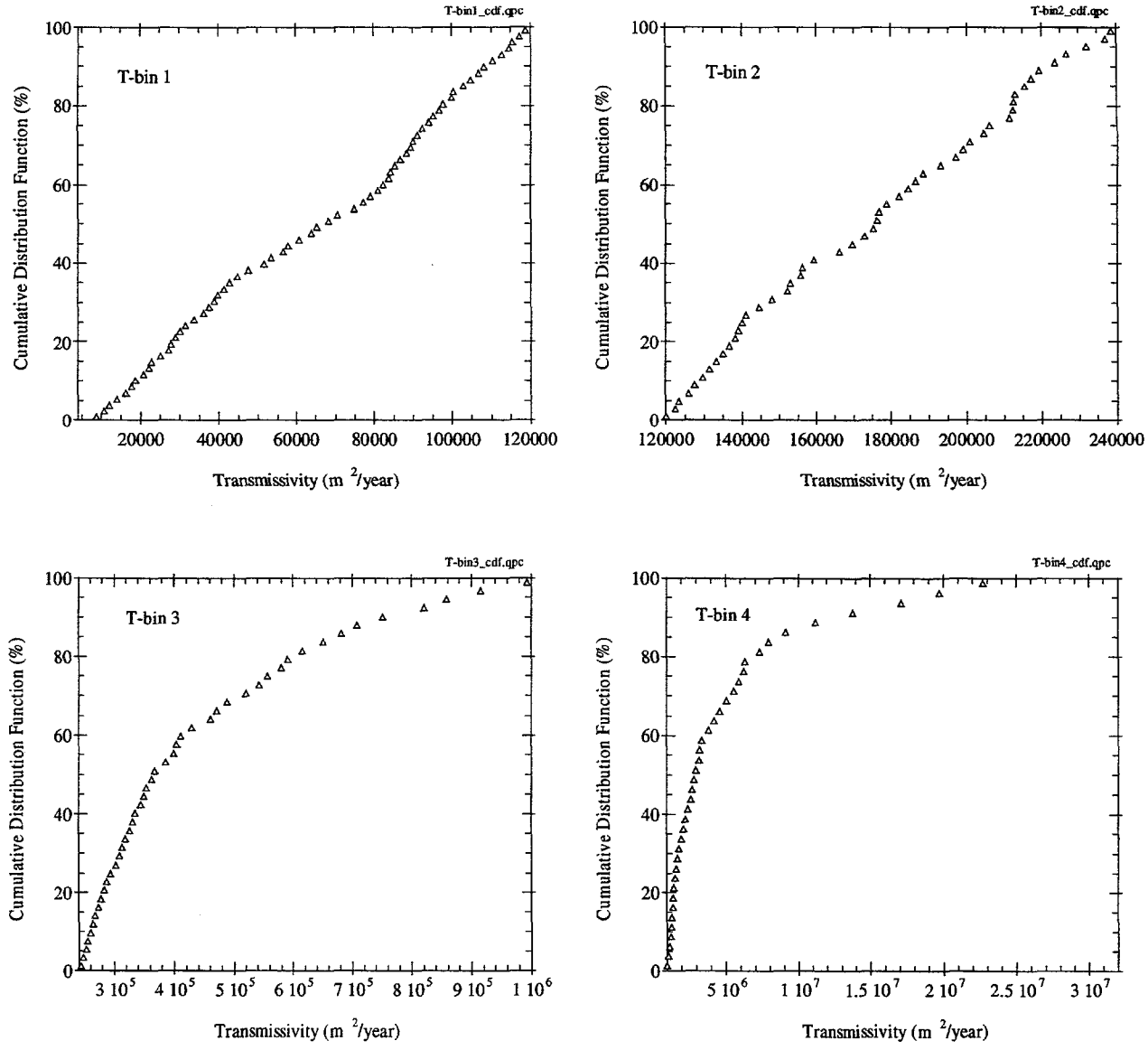

Figure 6. Cumulative distribution functions for four *T*-bins defined in saturated-zone PORFLOW model.

8. SATURATED-ZONE TRANSPORT PROPERTIES

The saturated-zone transport properties are identical to those defined for the vadose zone in Section 6. They include the distribution coefficient, K_d (m^3/kg), effective molecular diffusion coefficient, D_e (m^2/s), effective porosity, ϕ_e (-), longitudinal and transverse dispersivities, α_L and α_T (m), and bulk density, ρ_B (kg/m^3). These parameters are expressed in Equations (18)–(22) in Section 6.

8.1. Saturated-Zone Distribution Coefficients

In the Jacobs (1998) PORFLOW analysis, the distribution coefficients for the saturated zone was assumed to be equal to the far-field distribution coefficients used in the vadose zone. We recommend a similar approach by sampling a distribution coefficient from the far-field vadose-zone distributions given in Table 22 in Section 6.

8.2. Saturated-Zone Effective Molecular Diffusion Coefficient

The effective molecular diffusion coefficient is not expected to have a significant impact on the transport of radionuclides and performance of the site. As a result, a point estimate of 6.31×10^{-2} m^2/year as used by Jacobs (1998) is recommended for the saturated-zone model. This value is greater than the effective molecular diffusion coefficient used in the vadose zone because the tortuosity is reduced and the diffusive area is greater due to the saturated conditions.

8.3. Saturated-Zone Effective Porosity

The effective porosity, ϕ_e, in the saturated zone can affect the retardation factor of contaminants as expressed in Equation (19). In Jacobs (1998), two values of effective and total porosity were used in the saturated-zone PORFLOW model. Values of 25 percent for the effective porosity and 38 percent for the total porosity were assumed for a majority of the model corresponding to the upper Hanford unit. For the remainder of the model domain, values of 10 percent for the effective porosity and 36 percent for the total porosity were used.

In the MEPAS uncertainty analysis performed by Jacobs (1998), the total and effective porosities were assumed to be normally distributed (Table 5.4.10 in Jacobs, 1998). The statistics on the total porosity were obtained from the vadose-zone porosities in all soil categories reported in Khaleel and Freeman (1995). The ranges for the effective porosity were obtained from Hartman and Dresel (1998), and a mean value was assumed to be equal to the average of the upper and lower bounds. The standard deviation was calculated by assuming that the upper and lower bounds were equal to 3.33 standard deviations from the mean. For the LHS/PORFLOW analysis, we recommend using these distributions for the stochastic simulations as shown in Table 25. Point estimates that correspond to the Jacobs (1998) PORFLOW analysis are also included in Table 25.

Table 25. Distributions for total and effective porosity in the saturated zone.

Parameter	Point Estimate		Distribu-tion	Mean	S.D.	Lower Bound	Upper Bound	Ref.
	Upper Hanford	Plio-Pleistocene, Upper Ringold, Middle Ringold						
Total Porosity, ϕ_t	0.38	0.36	normal	0.35	0.073	0.20	0.52	1
Effective Porosity, ϕ_e	0.25	0.10	normal	0.15	0.015	0.10	0.20	2

[1]Khaleel and Freeman (1995)
[2]Hartman and Dresel (1998)

8.4. Saturated-Zone Longitudinal and Transverse Dispersivities

The longitudinal and transverse dispersivities for the saturated zone model in Jacobs (1998) were assumed to be constant and equal to 90 m and 9 m, respectively. They acknowledge that the range in dispersivities can be quite large because of the scale-dependence of this parameter. In addition, precise values of dispersivity cannot be measured for the site, and determination of these parameters must rely on inverse modeling. For the purposes of the LHS/PORFLOW analyses, we propose the following distribution shown in Table 26. A range of 0 to 180 m is assumed for the longitudinal dispersivity with a mean of 90 m. The standard deviation is determined by assuming the upper and lower bounds are three standard deviations from the mean. For consistency with the Jacobs (1998) analysis, the transverse dispersivity is calculated as ten percent of the longitudinal dispersivity (i.e., $\alpha_T = 0.1\ \alpha_L$).

Table 26. Longitudinal dispersivities for the model layers defined in Jacobs (1998) for the PORFLOW analysis. The point estimates are from Table 5.2.2 in Jacobs (1998).

Parameter	Mean	S.D.	Lower Bound	Upper Bound	Distribution
Longitudinal Dispersivity, α_L (m)	90	30	0	180	normal

8.5. Saturated-Zone Bulk Density

As defined in Section 6.5., the bulk density is equal to the mass of solid divided by the total volume occupied by solid, liquid, and gas. It is a function of the particle density, ρ_p, and the total porosity, ϕ_t, and is expressed in Equation (24). The particle density is assumed to be constant and equal to 2650 kg/m^3 for the entire saturated-zone PORFLOW model (Jacobs, 1998). Therefore, the variable in the bulk density will result from variations in the total porosity (see Table 25).

9. DISCUSSION

This section presents a discussion of issues that are relevant to modeling of contaminant transport at the AX Tank Farm. Many of the issues are raised as a result of reviews of the Retrieval Performance Evaluation Report (Jacobs, 1998). These points of discussion are intended to serve as a basis for improving and complementing the existing Jacobs' models.

9.1. Geological Conceptualization Issues

The geological conceptualization in Figure 5.2.2. of Jacobs (1998) is the basis for the vadose-zone flow and transport modeling effort. An evaluation of pertinent geological issues is presented here as a result of reviews of Jacobs (1998), Jones et al. (1998), and notes related to the work in the area of one of the authors (Smith, 1993). A summary of these observations is as follows:

1. A fuller analysis of the subsurface geology and uncertainty in the knowledge of that geology would require consultation of primary data sources, principally borehole lithologic logs.

2. From a process-sedimentology perspective, and in the absence of constraining primary data, a simple realization of continuous tabular layers for the principal hydrostratigraphic units can be justified, as used in the flow model (see Figure 2).

3. The inclusion of strong anisotropy in the flow models is geologically substantiated by the layering of the deposits at the meter scale, including alternation of material with strongly contrasting hydraulic properties at that scale.

4. It is geologically reasonable to simulate clastic dikes as preferential-flow pathways within a flow realization.

9.1.1. Need for Primary Data

The conceptualization represented in Figure 5.2.2. of Jacobs (1998) is purportedly based on a synthesis of several studies that summarize borehole stratigraphy in this part of the 200E Separation Area. These include at least 23 dry wells drilled at the 241 AX tank farm. Future modeling efforts would likely be enhanced by consultation of the available borehole logs and the reports summarizing their contents in order to (a) evaluate the level of uncertainity represented in the Jacobs (1998) conceptualization; (b) produce additional cross-sections to evaluate 3-dimensional variability; and (c) produce a 3-dimensional, rather than 2-dimensional, hydrostratigraphic model, if desired. The possibility of success in accomplishing these latter two activities should be tempered by consideration of the inconsistent quality and reliability of borehole data for this site (Jones et al., 1988, p. A-3; K. Lindsey, D.B. Stephens and Associates, telephone communication, Sept. 1998). Nonetheless, if such inconsistencies and variable resolution lead to significant uncertainity in the construction of any cross-section (e.g., Figure

5.2.2. of Jacobs, 1998), it would be useful to attempt to capture that uncertainity in some fashion prior to flow simulation.

9.1.2. Continuity of Tabular Layers

The simple, tabular distribution of the principal hydrostratigraphic units used in the flow simulations by Jacobs (1998) can be geologically justified. Most of the unsaturated zone is within the Hanford formation. These strata were deposited by many catastrophic late Pleistocene glacial-outburst floods originating at Glacial Lake Missoula in western Montana. The details of catastrophic-flood-deposit stratigraphy at the Hanford Site remains poorly known and a complex facies relationship is implied. Nonetheless, it is apparent that, because of the catastrophic discharges of the floods, assessment of the stratigraphy by utilization of traditional fluvial facies associations and facies geometries is inappropriate (Smith, 1993).

Although general lateral trends in grain size (and hence hydraulic properties) are known to be present, observations of Hanford formation in transient excavation exposures around the 200 Areas plateau indicate that layering is remarkably tabular and continuous over distances of many tens of meters. For example, meter-scale layers can be correlated nearly one-for-one over a distance of about 100 m at the U.S. Ecology site, approximately 3.8 km southwest of the 241 AX tank farm (Smith, 1993, p. 90-91). The shape assigned to hydrostratigraphic unit 2 in the Jacobs (1998) conceptualization and, particularly, the depiction of a 3.5-m wide, 4.8-m thick upward projection of gravel within that unit, is not representative of outcrop characteristics.

At the meter to tens-of-meters scale, contacts between sand and gravel are rarely gradational within exposures of the Hanford formation. The depiction of gradational, interfingering ("shazam-line") contacts between sand-dominated and gravel-dominated units in Figure 5.2.2. of Jacobs (1998) is a traditionally accepted way of representing uncertainity in contact relationships between contrasting sediment types encountered in adjacent, but separated, boreholes. Analogue outcrops in transient exposures at Hanford suggest, however, that such interfingering is unlikely, in this case.

Simplification of hydrostratigraphic units to more tabular shapes is, therefore, geologically justified but it would be useful to know how well this interpretation is constrained by well data. In addition, the distribution of hydrologic properties within these continuous tabular units may varied, as discussed in Section 9.2.2.

9.1.3. Meter-Scale Anisotropy

Although the traditional subdivision of the Hanford formation (e.g., units H1, H2, H3) captures the larger-scale distribution of dominant grain sizes, meter-scale interbedding of sediment with contrasting texture is known to dominate some intervals and should be expected to impart a strong anisotropy. At the U.S. Ecology site, for example (Smith, 1993), the H2 deposits are seen to be composed of rhythmic alternations of coarse pebbly sand (20 cm to 1.1 m thick) and fine silty sand (5-20 cm thick) (see Figure 7). The fine-grained layers are continuous for hundreds of meters. Soil horizons and loess layers are also known to intervene between coarser flood deposits (Smith, 1993). Jones et al. (1998, p. B-5) cite a vadose-zone-flow-path experiment in the 200E Area that was dominated by horizontal flow. In the context of Jones et al.'s (1998)

interpretation of this phenomenon, it is likely that persistant dry, fine grained layers have high conductivities at high tension, favoring lateral flow of fluid. The inclusion of a strong anisotropy in flow simulations is justified, therefore, both because there are experimental data near the 241 AX tank farm showing that such conditions exist and there is a geological rationale for anticipating the phenomenon.

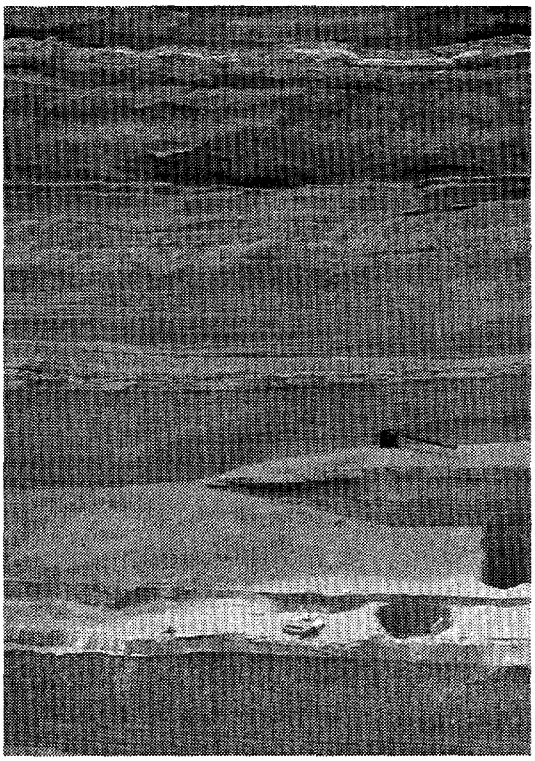

Figure 7. Photograph of excavation at U.S. Ecology site showing layering in Hanford formation H2. Dark, laminated layers are principally coarse, pebbly sand; lighter colored resistant layers are silty fine sand; white layer near top is a volcanic ash bed.

9.1.4. Clastic Dikes

Clastic dikes are ubiquitous features of the Hanford Formation that may provide vertical conduits for flow under the AX tank farm. Observations at the U.S. Ecology site show clastic dikes to be 10 cm to 2 m wide and spaced at ~10-35-m intervals (Figure 8). They have a strong vertical fabric of alternating sandy and silt-and-clay-rich bands, each up to several centimeters wide. The outermost vertical band, bordering horizontally layered sediment, is always clay rich. It is probably unlikely that more than one clastic dike would be present within any single cross-section of the 241 AX tank farm but there is probably a high probability that at least one such dike is present (this probability might be more rigorously assessed by consultation of reports by the DOE's contractors at Hanford who have studied the distribution of these features). There is a

reasonable geologic basis, therefore, for performing flow simulations through a strongly layered vadose zone that contains a vertical barrier to lateral flow that may also serve as vertical pathway for flow could be compared to a simulation lacking such a feature.

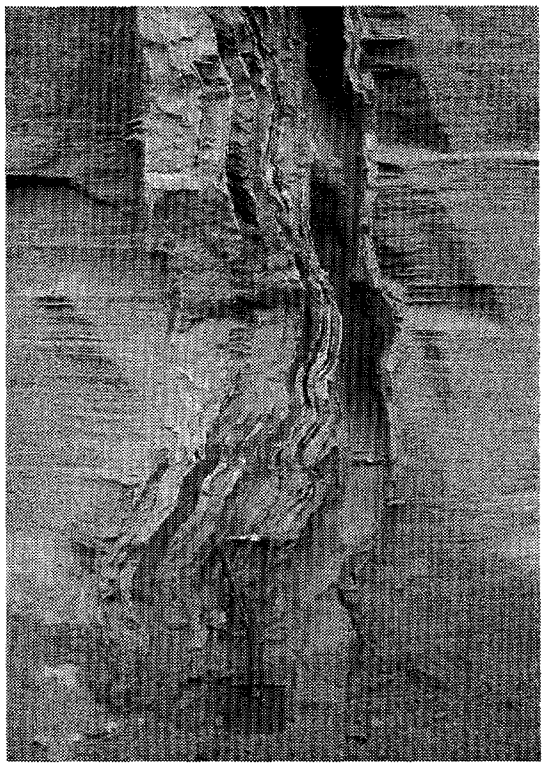

Figure 8. Photograph of clastic dike at U.S. Ecology site. Note multiple vertical layers and truncation of horizontal layering. Clay-rich bands in dike are lighter colored and more resistant; darker sandy layers are more recessed because of lack of cohesion.

9.2. Vadose-Zone Modeling Issues

To satisfy the intent of coupling LHS and PORFLOW, distributions of vadose zone hydrologic properties have been identified and developed in this report. The development of these stochastic distributions, while potentially providing some useful insights into the propagation of conceptual model uncertainties in contaminant transport predictions, are constrained by the assumption of idealized homogeneous strata. In addition, other potentially more significant aspects of model uncertainty have not been addressed at this point.

Based on the knowledge gained from the information presented in the draft Retrieval Performance Evaluation (RPE) report (Jacobs, 1998), a number of additional aspects contributing to model uncertainty have been identified. These components contributing to uncertainty can be grouped into three general categories:

1. fluid properties and fluid-sediment interactions

2. conceptual representation of the hydrostratigraphic setting

3. scenario definition and numerical modeling approximations

9.2.1. Fluid Properties and Fluid-Sediment System

In this category, there are three important modeling issues. The first is the simplifying (and implicit) assumption that water flow in porous media mimics the fluid flow characteristics of the residual liquid (i.e., sodium nitrate supernatant liquid) in the Hanford vadose zone. This is potentially a non-conservative assumption because the chemical properties (e.g., high pH) of the residual liquid are such that it can alter the physical structure of the porous media in the vicinity of the tank leak, resulting in the formation of macro-pores and enhanced fluid flow. These exotic chemical interactions (and elevated temperature) of the fluid and media, are neglected in the present and previous modeling studies. Certain fluid-sediment interactions may not need to be explicitly modeled for the RPE studies; however, these geochemical interactions need to be carefully examined through a combination of theoretical and experimental studies to estimate their effect on predictions of contaminant plume movement

Similarly, the analyses conducted here, and in the Jacobs (1998) report, assume that the unsaturated hydraulic data obtained for water-sediment samples is sufficiently representative of the hydraulic properties of a residual liquid-sediment system. Considering the fact that the HLW liquid is 3 to 8 times more viscous than water, about 40% more dense than water, and probably a non-Newtonian fluid, the moisture retention curve (i.e., capillary pressure versus moisture content) and the hydraulic conductivity curve (i.e., unsaturated hydraulic conductivity versus moisture content or capillary pressure) data for the water-sediment system should not be reasonably expected to be even roughly similar to those for the residual liquid-sediment system.

In addition to the above physical effects of fluid-sediment interactions, the chemical effects appear to impact the fluid and media properties. For example, chemical reactions can result in changes in the sorption properties in a manner that increases the mobility of important radionuclides such as Cesium-137. For example, radionuclide transport is likely to have been impacted by the high sodium nitrate solution in tank waste that leaked from the tanks. Since sodium concentrations in the tank waste is five to six orders of magnitude higher than cesium concentrations and both cesium and sodium compete for the same ion exchange sites, the sorptive capacity of soils for cesium would likely be substantially lowered in the presence of high sodium concentrations. The deterministic treatment of near-field and far-field distribution coefficients may overestimate the sorptivity in any given region. In addition, the high salt concentration in the fluid could potentially induce osmotic effects that could induce water flow and water-vapor movement towards the contaminant plume, resulting in increased moisture levels that would facilitate enhanced plume migration towards the saturated zone. Also, recognizing that the sludge layer in the SSTs are formed by particulates, it may be a source of colloidal particles that facilitate transport of sorbing radionuclides (e.g., Cesium-137); waste retrieval processes such as hydraulic sluicing could potentially cause resuspension of radiocolloids that could, in turn, migrate along with the aqueous phase radionuclides. Again, both theoretical and experimental studies are needed to examine the specific impact (i.e.,

predictive error) of the fluid-media property assumption and fluid-sediment chemical interactions.

9.2.2. Conceptual Representation of the Hydrostratigraphic Setting

For the purposes of numerical modeling, it is most convenient to represent the hydrostratigraphic setting as a simple tabular geology composed of homogeneous layers representing the various geologic formations. Such an idealization of the vadose zone, although convenient, will generally bias plume calculations in a non-conservative direction. Although a geologic rationale for the existence of tabular units has been discussed, the database from Khaleel and Freeman (1995) indicates considerable intra-facies variation in hydrologic properties. Therefore, a more realistic representation of the hydrostratigraphy might entail generating random fields for hydraulic properties within each unit. Flow and transport modeling based on generating random property fields is computationally intensive. However, this approach could yield more meaningful simulations of subsurface plume migration as well as provide a reference from which to judge to the utility of the more idealized representation currently being used. Geostatisical methods could be employed as an alternative to LHS to generate intra-unit heterogeneities to determine the potential impact of heterogeneous hydraulic properties within units.

In addition to accounting for the spatial variability of hydraulic properties, the conceptual representation should more realistically account for other localized, discrete features such as clastic dikes and sills. Since the locations and dimensions of these features are not well known, their placement within the geologic/hydrostratigraphic field of the model should be random (either based on spatial statistics or some additional understanding of how and where these features form). Additionally, there seems to be uncertainty concerning appropriate hydraulic properties to be assigned to these features. Clastic dikes have been proposed as preferential flow paths and also as barriers to flow. Based on this high degree of uncertainty, the assignment of hydraulic properties should be made using a statistical sampling procedure that captures the entire range of potential hydraulic properties. In this manner, stochastic simulations can bound the range of possible effects of these discrete features on the contaminant plume geometry and transport rates.

9.2.3. Scenario Definition and Modeling Approximations

Predictions of contaminant plume movement are dependent on a number of aspects of the "leak scenario" and often implicit numerical approximations made in the computer model. Various characteristics that define the tank leak scenario include: (a) geometry of the source zone, (b) single versus multiple plumes, and (c) secondary sources of water flow. These determine both rate and extent of the radionuclide transport. Similarly, numerical approximations, such as those associated with calculating the interblock properties (i.e., hydraulic conductivity and soil moisture capacity at interfaces of finite difference grids) and the discretization of the hydrostratigraphy can have a non-negligible impact on the calculated rate of plume migration.

In the case of a leak scenario, for example, a source rate specified over a significant portion of the tank base will generally exhibit much less downward movement than a leak occurring over a narrow crack, for the case of the same source rate. In addition, from hydraulic considerations, one should expect the crack geometry (i.e., horizontal versus vertical crack) might produce very

distinct plume patterns. Along with crack geometry, assuming a single plume and isolated plume will under-estimate the more plausible situation involving the coalescing of multiple plumes from multiple cracks in a single and/or adjacent SSTs. In addition, the impact of any possible secondary sources of water (e.g., surface runoff flowing into dry-wells, drainage from tile fields, leaks from pipelines) need to be assessed to ensure a properly bounded calculation of contaminant plume migration.

In the case of numerical approximations, finite difference codes (such as PORFLOW) require the user to specify the algorithm (e.g., upwinding, geometric mean, harmonic mean) to be used in calculating interblock hydraulic properties. There is considerable information in the technical literature that indicates that different algorithms for the interblock property calculation can produce dramatically different rates of wetting front (i.e., plume front) movement. In addition, codes limited to using rectangular finite difference grids are restricted to represent hydrostratigraphic units of variable thickness in a stair-step manner. The effect of this grid approximation is that it results in neglecting the gravity component along the dip angle; overall, this approximation can produce plume calculations that underestimate the rate of plume migration. Finally, the need to scale source terms to accommodate reduced dimensionality models should be evaluated with comparisons to full-dimensionality models.

9.2.4. Sufficiency of Modeling Conservatism

The RPE selected modeling approach permitted the consideration of many alternative options. In some ways, the RPE vadose-zone model represented an enhancement over previous Hanford studies with the implementation of a two-dimensional domain, incorporation of a clastic dike, and the notion of chemically altered mobility. In other ways, its conceptualization has included some simplistic assumptions related to the physical setting, physiochemical processes, and the release scenarios. Such simplifications could be considered in future probabilistic analysis combined with field characterization to minimize the chance of producing misleading calculations.

The following are assumptions presented in the draft RPE report (Jacobs, 1998) that may need further evaluation to assure a sufficient level of conservatism:

- Distributing the retrieval and residual leak sources over large portions of the tank base rather than focusing leaks in point sources. The data are limited and quantifying the impact of this assumption may best be handled stochastically or with sensitivity analysis.

- Placing the possible fast path features (e.g., clastic dikes) in between the tanks. There are no data on clastic dike locations within the AX Tank Farm. Sensitivity analysis with respect to the clastic dike location should be considered as a precursor to potential field investigations.

- Assigning hydraulic properties to the clastic dikes that are not significantly different from the surrounding sediments. This in fact may be an appropriate assumption given that the clastic dikes consist of the surrounding sediments. However, additional field studies may be warranted.

- Assuming that each geologic layer is homogeneous. The Site data are limited and there are no AX Tank Farm-specific data concerning homogeneity. Quantifying the impact of this assumption may best be handled stochastically or with sensitivity analysis.

- Using non-zero distribution coefficients for I-129 and C-14. This is an example of using best-estimate values instead of bounding estimates. This assumption is based on emerging information (Kincaid et al., 1998); however, the potential impact that this assumption has on the decision process should be determined with a sensitivity analysis.

These assumptions may collectively introduce a large margin of non-conservatism into the analyses. In expressing this concern, however, it is acknowledged that the proper degree of conservatism is a subjective decision. One approach to making these decisions would be to elicit opinions from independent PA experts and to conduct detailed evaluations of model uncertainty through stochastic analyses.

9.3. Saturated-Zone Modeling Issues

The current model of the saturated zone assumes a two-dimensional horizontal domain that is one meter thick. Although this assumption may provide conservative estimates of contaminant concentrations, the use of a constant one meter thick saturated zone may be too conservative. One would expect the plume to continually spread vertically throughout the saturated zone due to mechanical and molecular dispersion. Confinement of the contaminant plume to a one meter thick boundary layer over thousands of meters seems unrealistic.

There appears to be a paucity of data for saturated-zone parameters—or at least there appears to be a need for a comprehensive database of parameters and distributions for the saturated zone. A compilation of saturated-zone parameters similar to that of Khaleel and Freeman (1995) for vadose-zone parameters would be very beneficial for saturated-zone simulations of the Hanford AX Tank Farm.

10. CONCLUSIONS

Parameter distributions have been developed for stochastic simulations of flow and transport at the Hanford AX Tank Farm using PORFLOW and LHS. The stochastic parameters have been categorized into six groups: (1) source term, (2) infiltration/recharge, (3) vadose-zone hydrologic properties, (4) vadose-zone transport properties, (5) saturated-zone hydrologic properties, and (6) saturated-zone transport properties.

For the source term, contaminant leaks were categorized into past leaks, retrieval leaks, and residual leaks. Stochastic distributions of the leak volume and contaminant concentrations were presented for the past leaks and retrieval leaks, and distributions for the inventory and solubilities were presented for the residual leak.

The infiltration rates at the Hanford AX Tank Farm were categorized into the following periods: pre-tank (before 1963), current conditions (1963-2020), surface barrier conditions (500 to 1000 years after 2020), and post-surface barrier conditions. Distributions for the infiltration rates during each of these periods was provided based on estimates reported in Jacobs (1998).

The vadose-zone hydrologic properties that were considered included residual and saturated moisture contents, van Genuchten α and n parameters, and saturated conductivity. Distributions were taken from Khaleel and Freeman (1995), and a rank regression analysis was performed on each of the parameters. No strong correlation was found to exist, so it was recommended that the sampling of the parameters be performed independently.

The vadose-zone transport properties that were considered included the distribution coefficients of four radionuclides, effective molecular diffusion coefficient, longitudinal and transverse dispersivities, effective porosity, and bulk density. A deterministic point estimate was recommended for the effective molecular diffusion coefficient, but distributions for all other parameters were developed from sources provided in Kincaid et al. (1998) and Jacobs (1998) or through expressions relating the transport properties to vadose-zone hydrologic parameters.

The only saturated-zone hydrologic parameter that was evaluated was the effective conductivity or transmissivity. The transmissivity values for 200 materials used in the PORFLOW model (Jacobs, 1998) were lumped into four bins, and cumulative distribution functions for each bin were developed for use in LHS. It was recommended that all materials in PORFLOW belonging to a bin use the same sampled transmissivity value to reduce the number of realizations required.

Finally, the same transport properties identified in the vadose zone were examined for the saturated zone as well. The distribution coefficients identified for the far-field in the vadose zone were recommended for the saturated zone. In addition, the distribution of total porosities for all soil categories in the vadose zone (Khaleel and Freeman, 1995) was used for the saturated-zone porosities. A distribution for the effective porosity was taken from Jacobs (1998). A normal distribution for the dispersivities was developed based on the deterministic value used

in Jacobs (1998), and the bulk density was expressed as a function of the total porosity. The effective molecular diffusion coefficient was assumed constant.

The parameters that were developed in this report will be used to perform stochastic simulations using the state-of-the-art multiphase simulator PORFLOW coupled with the Latin Hypercube Sampling method. The objective of these simulations is to provide additional uncertainty analyses that complement the existing Jacobs' models of flow and transport at the Hanford AX Tank Farm.

REFERENCES

ACRI (Analytic & Computational Research Inc.), 1997, *PORFLOW User's Manual*, version 4.00, Bel Air, CA.

Devore, J.L., 1982, *Probability & Statistics for Engineering and the Sciences*, Brooks/Cole Publishing Co., Monterey, CA.

Domenico, P.A. and F.W. Schwartz, 1990, *Physical and Chemical Hydrogeology*, John Wiley & Sons, New York, NY.

Hartman, M.J. and P.E. Dresel, eds., 1998, Hanford Site Groundwater Monitoring for Fiscal Year 1997, *PNNL-11793*, Pacific Northwest National Laboratory, Richland, WA.

Jacobs, 1998, Retrieval Performance Evaluation Report (draft), Jacobs Engineering Group, Richland, WA, August 1998.

Jones, T.E., R. Khaleel, D.A. Myers, J.W. Shade, and M.I. Wood, 1998, TWRS Vadose Zone Conceptual Model and Assessment of Critical Data Gaps (draft), *HNF-2603*.

Khaleel, R. and E.J. Freeman, 1995, Variability and Scaling of Hydraulic Properties for 200 Area Soils, Hanford Site, *WHC-EP-0883*, Westinghouse Hanford Company, Richland WA.

Kincaid, C.T., M.P. Bergeron, C.R. Cole, M.D. Freshley, N.L. Hassig, V.G. Johnson, D.I. Kaplan, R.J. Serne, G.P. Streile, D.L. Strenge, P.D. Thorne, L.W. Vail, G.A. Whyatt, S.K. Wurstner, 1998, Composite Analysis for Low-Level Waste Disposal in the 200 Area Plateau of the Hanford Site, *PNNL-11800*, Pacific Northwest National Laboratory, Richland, WA.

NHC, 1997, AX Tank Farm Waste Inventory Study for the Hanford Tanks Initiative Project, *HNF-SD-HTI-TI-001*, Rev. 0, Numatec Hanford Corporation, Richland, WA.

Piepho, M.G., J.P. Davis, K.A. Lindsey, M.D. Ankeny, and M.A. Prieksat, Sensitivity Analyses of Sluicing-Leak Parameters for the 241-AX Tank Farm, WHC-SD-WM-ANAL-052, Rev. 0, Westinghouse Hanford Company, Richland, WA.

Rockhold, M.L., M.J. Fayer, C.T. Kincaid, and G.W. Gee, 1995, Estimation of Natural Ground Water Recharge for the Performance Assessment of a Low-level Waste Disposal Facility at the Hanford Site, *PNL-10508*, Pacific Northwest National Laboratory, Richland, WA.

Schramke, J.A., C.S. Glantz, and G.R. Holdren, 1994, Hanford Site Environmental Setting Data Developed for the Unit Risk Factor Methodology in Support of the Programmatic Environmental Impact Statement (PEIS), PNL-9801, Pacific Northwest National Laboratory, Richland WA.

Smith, G.A., 1993, Missoula Flood Dynamics and Magnitudes Inferrred from Sedimentology of Slack-Water Deposits on the Columbia Plateau, Washington, *Geological Society of America Bulletin*, v. 105, p. 77-100.

van Genuchten, M.Th., 1980, A Closed-Form Equation for Predicting the Hydraulic Conductivity of Unsaturated Soils, *Soil Science Society of America Journal*, Vol. 44, pp. 892-898.

Walton, W.C., 1985, Practical Aspects of Groundwater Modeling, National Water Well Association, Worthington, OH.

Wyss, G.D. and K.H. Jorgensen, 1998, A User's Guide to LHS: Sandia's Latin Hypercube Sampling Software, *SAND98-0210*, Sandia National Laboratories, Albuquerque, NM.

APPENDIX A: HYDROLOGIC PARAMETERS FROM KHALEEL AND FREEMAN (1995)

Sieve Analysis																sampling	
Site	sample no.	borehole	depth (m)	gr	cs	fs	silt	clay	soil type #	formation	alpha (1/cm)	n	theta_r	theta_s	Ks (cm/s)	technique	Source
200-BP-1 [2,4]	1-0526	299-E33-38	1.9	47	18	8	27	0	sandy gravel (5)	Hanford Gravel	0.0164	1.5448	0.0229	0.2144	2.00E-05	splitspoon	Hoffman, 1992
	1-0527	299-E33-38	15.1	42	50	8	0	0	sandy gravel (6)	Hanford Gravel	0.0255	1.6222	0.015 [f]	0.0773	5.70E-05	splitspoon	Relyea, 1995
	1-0528	299-E33-38	51.0	42	50	8	0	0	sandy gravel (6)	Hanford Sand	0.0045	1.8509	0.0105	0.0746	5.00E-04	splitspoon	"
	1-0529	299-E33-38	62.3	79	14	7	0	0	sandy gravel (6)	Hanford Gravel	0.0026	1.4909	0.0000	0.0557	4.20E-03	splitspoon	"
	1-0530	299-E33-38	57.1	0	60	35	5	0	sand (2)	Hanford Sand	0.0123	1.6899	0.0098	0.2663	7.10E-05	splitspoon	"
	1-0531	299-E33-38	57.9	-----	-----	N/A	-----	-----	sand (2)	Hanford Sand	0.0017	1.8438	0.0400 [f]	0.4863	2.10E-06	splitspoon	"
	1-0550	299-E33-40	14.0	63	32	5	0	0	sandy gravel (6)	Hanford Gravel	0.0037	1.4567	0.0000	0.0757	6.00E-04	splitspoon	"
	1-1133	216-B-61A	4.1	76	13	11	0	0	sandy gravel (6)	Hanford Gravel	0.0028	1.8847	0.0162	0.0781	1.80E-03	splitspoon	"
	1-1134	216-B-61A	5.8	55	24	13	8	0	sandy gravel (5)	Hanford Gravel	0.0034	1.6905	0.0322	0.1409	2.80E-03	splitspoon	"
	1-1136	216-B-61A	7.0	68	20	12	0	0	sandy gravel (6)	Hanford Gravel	0.0056	1.4945	0.0187	0.1043	4.00E-04	splitspoon	"
	1-1137	216-B-61A	8.8	38	49	13	0	0	sandy gravel (5)	Hanford Gravel	0.0139	1.4207	0.0210	0.1542	1.80E-05	splitspoon	"
	2-2244	216-B-49A	26.5	1	49	48	2	0	sand (2)	Hanford Sand	0.0135	2.0185	0.0270	0.2687	4.60E-05	splitspoon	"
	2-2253	216-B-49A	35.5	2	85	13	0	0	sand (2)	Hanford Sand	0.0205	1.7138	0.0308	0.2284	8.80E-05	splitspoon	"
	2-2258	216-B-43A	41.3	1	84	15	0	0	sand (2)	Hanford Sand	0.0373	1.7815	0.0271	0.2306	2.80E-05	splitspoon	"
	2-2261	216-B-49A	48.6	12	76	12	0	0	gravelly sand (4)	Hanford Sand	0.0410	1.6885	0.0303	0.2026	1.80E-04	splitspoon	"
	2-2271	216-B-57A	60.5	50	28	14	6	2	sandy gravel (5)	Hanford Gravel	0.0074	1.4319	0.0145	0.1636	1.40E-05	splitspoon	"
	2-2283	216-B-57A	13.9	6	83	11	0	0	sand (2)	Hanford Sand	0.0298	1.6757	0.0269	0.2005	2.10E-05	splitspoon	"
	2-2286	216-B-49A	14.9	0	4	92	3	1	sand (2)	Hanford Sand	0.0077	3.0137	0.0569	0.4712	6.30E-05	splitspoon	"
	2-2289	216-B-43A	51.4	4	84	12	0	0	sand (2)	Hanford Sand	0.0131	1.6351	0.0409	0.1968	1.30E-04	splitspoon	"
	2-2294	216-B-43A	61.4	39	33	17	7	4	sandy gravel (5)	Hanford Gravel	0.0051	1.4514	0.0066	0.2006	4.40E-05	splitspoon	"
	2-2297	216-B-57A	65.4	80	20	0	0	0	sandy gravel (6)	Hanford Gravel	0.0059	1.8562	0.0074	0.0641	4.10E-04	splitspoon	"
218-W-5 [2,4]	0-073	299-W7-9	20.3	0	27	54	10	9	loamy sand (1)	Hanford sand	0.0008	1.9785	0.0600 [f]	0.4134	N/A	splitspoon	"
	0-082	299-W7-9	24.5	2	38	47	8	5	sand (2)	Plio-Pleistocene	0.0064	1.7084	0.1483	0.3336	6.30E-04	splitspoon	"
	0-085	299-W7-9	26.9	0	50	37	5	8	sand (2)	Plio-Pleistocene	0.0049	2.1261	0.0578	0.2105	1.30E-04	splitspoon	"
	0-101	299-W7-9	31.8	0	85	8	2	5	sand (2)	Upper Ringold	0.0695	1.4447	0.0228	0.2082	2.10E-04	splitspoon	"
	0-104	299-W7-9	34.2	0	72	24	3	1	sand (2)	Upper Ringold	0.0849	1.3106	0.0000	0.2082	1.10E-03	splitspoon	"
	5-0001	299-W7-9	21.6	4	4	79	8	5	sand (2)	Palouse paleosol	0.0057	2.8152	0.0200 [f]	0.3727	1.40E-04	splitspoon	Relyea, 1995
	5-0002	299-W7-9	24.9	2	38	47	8	5	sand (2)	Plio-Pleistocene	0.0039	1.9321	0.0678	0.3454	1.32E-04	splitspoon	"
	5-0003	299-W7-9	43.2	0	74	22	1	3	sand (2)	Upper Ringold	0.0414	1.9382	0.0211	0.3004	1.80E-04	splitspoon	"

	5-0004	299-W7-9	30.3	0	58	30	7	5	sand (2)	Upper Ringold	0.0102	1.5737	0.0267	0.3256	1.65E-04	splitspoon	"
	5-0005	299-W7-9	21.1	0	0	73	22	5	sandy loam (1)	Palouse paleosol	0.0069	2.2430	0.0400 [f]	0.3851	6.70E-05	splitspoon	"
	5-0006	299-W7-9	19.9	0	27	54	10	9	loamy sand (1)	Hanford sand	0.0064	2.2593	0.0584	0.3274	N/A	splitspoon	"
	5-0007	299-W7-9	40.3	0	80	13	5	2	sand (2)	Upper Ringold	0.1308	1.7017	0.0231	0.3502	3.00E-03	splitspoon	"
218-W-5 [1,5]	W7-2-65	299-W07-02	19.8	35	38	11	16	0	silty sandy gravel (3)	Plio-Pleistocene	0.02102	1.4563	0.064	0.3752	6.80E-02	splitspoon	Bjornstad, 1990
	W7-2-94	299-W07-02	28.6	48	39	7	6	0	sandy gravel (5)	Upper Ringold	0.0557	1.9669	0.0223	0.2168	3.70E-02	splitspoon	"
	W7-2-154	299-W07-02	46.9	32	36	15	17	0	silty sandy gravel (3)	Middle Ringold	0.1027	1.3782	0.0150 [f]	0.3071	2.10E-02	splitspoon	"
	W7-2-219	299-W07-02	66.8	39	35	18	8	0	sandy gravel (5)	Middle Ringold	0.068	1.7788	0.0617	0.1594	2.70E-03	splitspoon	"
	W10-13-45	299-W10-13	13.7	0	62	33	5	0	sand (2)	Hanford Sand	0.0408	2.0672	0.0396	0.3915	5.80E-02	splitspoon	"
	W10-13-80	299-W10-13	24.4	64	25	6	5	0	sandy gravel (5)	Hanford Gravel	0.2758	1.3718	0.0367	0.1781	2.70E-02	splitspoon	"
241-T-106 [2,4]	3-0210	299-W10-196	3.1	48	30	22	0	0	sandy gravel (5)	Hanford gravel	0.0115	2.2692	0.0450	0.1854	1.00E-03	splitspoon	Relyea, 1995
	3-0213	299-W10-196	5.6	31	33	36	0	0	gravelly sand (4)	Hanford gravel	0.0040	2.4233	0.0494	0.2083	1.02E-03	splitspoon	"
	3-0279	299-W10-196	1.8	46	32	20	2	0	sandy gravel (5)	Hanford gravel	0.0061	2.1046	0.0337	0.1492	N/A	splitspoon	"
	3-0589	299-W10-196	25.5	2	56	42	0	0	sand (2)	Hanford sand	0.0040	2.0685	0.0575	0.3443	1.38E-05	splitspoon	"
	3-0667	299-W10-196	42.2	80	13	7	0	0	sandy gravel (6)	Middle Ringold	0.0115	1.3466	0.0000	0.0718	2.83E-05	splitspoon	"
	3-0668	299-W10-196	38.9	63	15	12	10	0	sandy gravel (5)	Middle Ringold	0.0023	1.5765	0.0100 [f]	0.1470	1.60E-03	splitspoon	"
	3-0682	299-W10-196	46.1	0	54	35	10	1	sand (1)	Middle Ringold	0.0128	2.0864	0.0519	0.4334	4.57E-05	splitspoon	"
	3-0688	299-W10-196	48.5	0	38	28	28	6	sandy loam (1)	Middle Ringold	0.0036	1.6568	0.0302	0.3230	N/A	splitspoon	"
	3-0689	299-W10-196	52.2	0	36	30	25	9	sandy loam (1)	Middle Ringold	0.0022	1.6651	0.0300 [f]	0.3208	N/A	splitspoon	"
	3-0690	299-W10-196	53.7	0	39	31	23	7	sandy loam (1)	Middle Ringold	0.0042	1.6376	0.0564	0.3683	6.55E-06	splitspoon	"
APTANK [1,5]	241-AP1G	N/A	N/A	38	58	3	1	0	sandy gravel (5)	Hanford sand	0.1018	2.9473	0.0212	0.2599	1.24E-03	excavation	Heller., 1989
	241-AP-2	N/A	N/A	0	68	26	3	3	sand (2)	Hanford sand	0.0309	3.0872	0.0994	0.519	5.97E-04	excavation	"
	241-AP-3	N/A	N/A	0	85	12	2	1	sand (2)	Hanford sand	0.0494	3.4878	0.062	0.4348	8.10E-04	excavation	"
	241-AP-4G	N/A	N/A	10	83	5	2	0	sand (2)	Hanford sand	0.0698	2.6694	0.0416	0.4162	1.87E-03	excavation	"
	241-AP-5	N/A	N/A	0	7	49	36	8	sandy loam (1)	Hanford sand	0.0108	1.4367	0.0268	0.4293	4.94E-05	excavation	"
	241-AP-6	N/A	N/A	1	36	43	14	6	loamy sand (1)	Hanford sand	0.0053	1.9484	0.068	0.4049	8.60E-05	excavation	"
C-018-H [2,4]	2-1169	699-48-77	8.1	14	40	44	2	0	gravelly sand (4)	Plio-Pliestocene	0.0076	2.5367	0.0569	0.3069	5.30E-03	splitspoon	Relyea, 1995
	2-1170	699-48-77	8.9	22	42	33	3	0	gravelly sand (4)	Plio-Pliestocene	0.0048	1.9770	0.0635	0.3011	1.30E-04	splitspoon	"
	2-1176	699-48-77	13.0	1	79	20	0	0	sand (2)	Plio-Pliestocene	0.0223	1.7587	0.0262	0.2230	2.00E-02	splitspoon	"

	2-1181	699-48-77	14.1	8	82	10	0	0	sand (2)	Plio-Pliestocene	0.0728	1.3096	0.0230	0.2147	8.20E-03	splitspoon	"
	2-1431	699-48-77A	20.6	------	-----	N/A	-----	-----	sand (2)	Plio-Pliestocene	0.0227	1.5859	0.0432	0.2346	1.80E-02	splitspoon	"
	2-1432	699-48-77A	27.6	51	30	15	4	0	sandy gravel (5)	Middle Ringold	0.0083	1.5938	0.0191	0.1128	1.40E-02	splitspoon	"
ERDF [2,6]	4-0637	699-36-63A	74.9	------	-----	N/A	-----	-----	sand (2)	Hanford sand	0.0261	3.2937	0.0278	0.3743	N/A	splitspoon	Relyea, 1995
	4-0642	699-35-69A	25.7	0	60	30	10	0	sand (2)	Hanford sand	0.0119	1.6727	0.0566	0.3513	N/A	splitspoon	Weekes and Borghese, 1994
	4-0644	699-35-69A	49.8	0	27	56	12	5	loamy sand (1)	Hanford sand	0.0069	2.2673	0.0828	0.3922	N/A	splitspoon	"
	4-0791	699-35-65A	63.2	0	50	50	0	0	sand (2)	Hanford sand	0.0217	2.4513	0.0303	0.3371	N/A	splitspoon	"
	4-0792	699-35-65A	75.4	70	21	8	1	0	sandy gravel (6)	Middle Ringold	0.0276	1.6636	0.0091	0.0825	N/A	splitspoon	"
	4-0855	699-35-66B	12.2	0	7	83	5	5	sand (2)	Hanford sand	0.0088	3.2652	0.0689	0.3936	N/A	splitspoon	"
	4-0973	699-35-68A	37.0	0	21	64	12	3	loamy sand (1)	Hanford sand	0.0169	2.0085	0.0190 [f]	0.3525	1.27E-04	splitspoon	"
	4-0983	699-35-68A	82.9	17	35	42	4	2	gravelly sand (4)	Upper Ringold	0.0156	2.0226	0.0100 [f]	0.3373	5.43E-05	splitspoon	"
	4-1011	699-35-69A	73.0	0	4	60	28	8	loamy sand (1)	Plio-Pleistocene	0.0042	1.5218	0.0450 [f]	0.4913	1.00E-05	splitspoon	"
	4-1012	699-35-69A	73.9	50	20	20	7	3	sandy gravel (5)	Middle Ringold	0.0062	1.6452	0.0100 [f]	0.1643	5.10E-05	splitspoon	"
	4-1013	699-35-69A	77.9	77	6	12	3	2	sandy gravel (5)	Middle Ringold	0.0064	1.6574	0.0214	0.1397	1.90E-07	splitspoon	"
	4-1056	699-32-72B	61.7	0	6	88	4	2	sand (2)	Hanford sand	0.0071	2.7253	0.0350 [f]	0.4288	N/A	splitspoon	"
	4-1057	699-32-72B	49.5	0	2	68	24	6	loamy sand (1)	Hanford sand	0.0046	2.2861	0.0890	0.4877	N/A	splitspoon	"
	4-1058	699-32-72B	64.7	0	1	41	43	15	loam (1)	Hanford sand	0.0029	1.5267	0.1023	0.5661	N/A	splitspoon	"
	4-1076	699-35-61A	76.4	0	75	25	0	0	sand (2)	Hanford sand	0.0235	2.0956	0.0265	0.3433	N/A	splitspoon	"
	4-1079	699-35-61A	90.9	65	24	11	0	0	sandy gravel (5)	Middle Ringold	0.0073	1.6668	0.0295	0.1236	1.30E-03	splitspoon	"
	4-1080	699-35-61A	93.5	63	24	10	3	0	sandy gravel (5)	Middle Ringold	0.0062	1.6601	0.0302	0.1316	3.30E-06	splitspoon	"
FLTF [1,5]	D02-10	N/A	<6.1	0	2	54	34	10	sandy loam (1)	Warden silt loam	0.0049	1.9773	0.0778	0.4531	1.20E-04	excavation	Gee et al., 1989
	D02-16	N/A	<6.1	0	2	63	25	10	sandy loam (1)	Warden silt loam	0.0035	2.4632	0.0820 [f]	0.4630	1.20E-04	excavation	Volk, 1993
	D04-04	N/A	<6.1	0	4	58	28	10	sandy loam (1)	Warden silt loam	0.0072	1.6501	0.0700 [f]	0.4508	1.20E-04	excavation	"
	D04-10	N/A	<6.1	0	3	58	30	9	sandy loam (1)	Warden silt loam	0.0066	1.7574	0.0800 [f]	0.4428	2.90E-04	excavation	"
	D05-03	N/A	<6.1	0	4	63	23	10	sandy loam (1)	Warden silt loam	0.0055	1.8647	0.0860 [f]	0.4332	2.90E-04	excavation	"
	D07-04	N/A	<6.1	0	3	58	30	9	sandy loam (1)	Warden silt loam	0.0051	1.9424	0.0820 [f]	0.4435	1.20E-04	excavation	"
	D08-15	N/A	<6.1	0	2	57	31	10	sandy loam (1)	Warden silt loam	0.0059	1.8533	0.0850 [f]	0.4543	1.20E-04	excavation	"
	D09-01	N/A	<6.1	0	3	51	37	9	sandy loam (1)	Warden silt loam	0.0066	1.7677	0.0800 [f]	0.4544	1.20E-04	excavation	"
	D09-02	N/A	<6.1	0	2	57	31	10	sandy loam (1)	Warden silt loam	0.0069	1.8498	0.0825	0.4559	1.20E-04	excavation	"
	D09-05	N/A	<6.1	0	7	60	29	4	sandy loam (1)	Warden silt loam	0.0088	1.6183	0.0681	0.4461	2.90E-04	excavation	"

	D10-04	N/A	<6.1	0	6	59	30	5	sandy loam (1)	Warden silt loam	0.0064	1.7899	0.0850 f	0.4481	1.20E-04	excavation	"
	D11-06	N/A	<6.1	0	4	57	33	6	sandy loam (1)	Warden silt loam	0.0061	1.8575	0.0850 f	0.4308	1.20E-04	excavation	"
	D11-08	N/A	<6.1	0	5	58	32	5	sandy loam (1)	Warden silt loam	0.0061	1.7567	0.0850 f	0.4312	1.20E-04	excavation	"
	D12-14	N/A	<6.1	0	3	52	34	11	sandy loam (1)	Warden silt loam	0.0063	1.7576	0.0980 f	0.4686	1.20E-04	excavation	"
	D13-08	N/A	<6.1	0	4	52	35	9	sandy loam (1)	Warden silt loam	0.0070	1.7877	0.0820 f	0.4513	1.20E-04	excavation	"
	D14-04	N/A	<6.1	0	3	56	36	5	sandy loam (1)	Warden silt loam	0.0065	1.8553	0.0837	0.4586	1.20E-04	excavation	"
GROUT [1,5]	5A	299-E25-234	1.5	1	73	17	5	4	sand (2)	Eolian sand	0.1480	1.3087	0.0187	0.4131	5.73E-04	splitspoon	Rockhold et al., 1993
	5B	299-E25-234	1.5						sand (2)	Eolian sand	0.0211	1.5360	0.0336	0.3367	5.73E-04	splitspoon	"
	19A	299-E25-234	5.8	2	28	53	12	5	loamy sand (1)	Eolian sand	0.3870	1.2615	0.0461	0.4860	8.88E-04	splitspoon	"
	19B	299-E25-234	5.8						loamy sand (1)	Eolian sand	0.2729	1.5326	0.0363	0.5026	8.88E-04	splitspoon	"
	25A	299-E25-234	7.6	0	49	36	10	5	loamy sand (1)	Eolian sand	0.0473	2.0595	0.0539	0.4407	1.80E-03	splitspoon	"
	25B	299-E25-234	7.6						loamy sand (1)	Eolian sand	0.0519	1.3421	0.0342	0.5228	1.80E-03	splitspoon	"
	25C	299-E25-234	7.6						loamy sand (1)	Eolian sand	0.0287	1.3529	0.0280 f	0.5062	1.80E-03	splitspoon	"
	25D	299-E25-234	7.6						loamy sand (1)	Eolian sand	0.0700	1.8780	0.0800 f	0.4822	1.80E-03	splitspoon	"
	29A	299-E25-234	8.8	0	60	31	6	3	sand (2)	Eolian sand	0.2718	1.1928	0.0000	0.4341	2.41E-05	splitspoon	"
	29B	299-E25-234	8.8						sand (2)	Eolian sand	0.1033	1.2242	0.0000	0.4387	2.41E-05	splitspoon	"
	37A	299-E25-234	11.3	1	43	39	10	7	loamy sand (1)	Eolian sand	0.0775	1.2921	0.0703	0.5114	5.77E-04	splitspoon	"
	37B	299-E25-234	11.3						loamy sand (1)	Eolian sand	0.0914	1.3319	0.0844	0.5304	5.77E-04	splitspoon	"
	46A	299-E25-234	14	0	73	22	2	3	sand (2)	Hanford sand	0.2923	1.3658	0.0000	0.4581	2.99E-04	splitspoon	"
	46B	299-E25-234	14						sand (2)	Hanford sand	0.0613	1.4343	0.0000	0.3708	2.99E-04	splitspoon	"
	54A	299-E25-234	16.5	1	51	32	9	7	loamy sand (1)	Hanford sand	0.1524	1.4137	0.0262	0.4488	1.38E-05	splitspoon	"
	54B	299-E25-234	16.5						loamy sand (1)	Hanford sand	0.1451	1.4419	0.0216	0.4543	1.38E-05	splitspoon	"
	69A	299-E25-234	21	3	71	19	5	2	sand (2)	Hanford sand	0.3357	1.2658	0.0000	0.3721	1.21E-03	splitspoon	"
	69B	299-E25-234	21						sand (2)	Hanford sand	0.2269	1.6572	0.0288	0.4042	1.21E-03	splitspoon	"
	83A	299-E25-234	25.3	4	70	19	5	2	sand (2)	Hanford sand	0.2979	1.3300	0.0070 f	0.3915	1.78E-04	splitspoon	"
	83B	299-E25-234	25.3						sand (2)	Hanford sand	0.1157	1.4027	0.0070 f	0.3696	1.78E-04	splitspoon	"
	99A	299-E25-234	30.2	0	34	60	4	2	sand (2)	Hanford sand	0.7417	1.2557	0.0000	0.3692	2.24E-04	splitspoon	"
	99B	299-E25-234	30.2						sand (2)	Hanford sand	0.3823	1.3262	0.0100	0.3765	2.24E-04	splitspoon	"
	110A	299-E25-234	33.5	6	64	23	5	2	sand (2)	Hanford sand	0.1964	1.8193	0.0324	0.4293	2.82E-04	splitspoon	"
	110B	299-E25-234	33.5						sand (2)	Hanford sand	0.1991	1.8015	0.0326	0.4201	2.82E-04	splitspoon	"
	117A	299-E25-234	35.7	3	62	26	5	4	sand (2)	Hanford sand	0.1114	1.6538	0.0259	0.4538	3.63E-03	splitspoon	"
	117B	299-E25-234	35.7						sand (2)	Hanford sand	0.0230	1.5237	0.0011	0.3831	3.63E-03	splitspoon	"

	126A	299-E25-234	38.4	51	33	14	1	1	sandy gravel (5)	Hanford sand	0.9193	1.3700	0.0106	0.1755	1.98E-03	splitspoon	"
	126B	299-E25-234	38.4						sandy gravel (5)	Hanford sand	0.4783	1.4639	0.0127	0.1823	1.98E-03	splitspoon	"
	133A	299-E25-234	40.5	30	33	25	9	3	silty sandy gravel (3)	Hanford sand	0.0163	1.3134	0.0000	0.1877	2.76E-05	splitspoon	"
	133B	299-E25-234	40.5						silty sandy gravel (3)	Hanford sand	0.0331	1.2555	0.0000	0.1871	2.76E-05	splitspoon	"
Injection [2,4]	1-1417	299-E24-95	1.8	1	23	68	7	1	sand (2)	Hanford sand	0.0051	1.6827	0.0200 [f]	0.3501	1.40E-04	core barrel	Relyea, 1995
	1-1418	299-E24-95	3.0	18	56	26	0	0	gravelly sand (4)	Hanford sand	0.0310	1.5289	0.0336	0.2152	1.80E-04	core barrel	"
	1-1419	299-E24-95	4.9	2	88	10	0	0	sand (2)	Hanford sand	0.4984	1.4065	0.0090	0.3013	3.20E-04	core barrel	"
	2-1636	299-E24-95	4.9	2	84	14	0	0	sand (2)	Hanford sand	0.1385	1.7079	0.0228	0.3073	8.70E-04	core barrel	"
	2-1637	299-E24-79	9.8	0	80	20	0	0	sand (2)	Hanford sand	0.0760	1.8863	0.0248	0.3026	4.20E-03	core barrel	"
	2-1638	299-E24-79	12.2	0	81	19	0	0	sand (2)	Hanford sand	0.1016	1.3365	0.0000	0.2720	5.80E-03	core barrel	"
	2-1639	299-E24-79	18.3	0	93	7	0	0	sand (2)	Hanford sand	0.3333	1.5801	0.0179	0.3206	1.30E-03	core barrel	"
	2-2225	299-E24-92	9.8	0	80	20	0	0	sand (2)	Hanford sand	0.0242	4.1695	0.0335	0.3309	5.50E-03	core barrel	"
	2-2226	299-E24-92	15.2	6	90	4	0	0	sand (2)	Hanford sand	0.5282	1.4780	0.0168	0.2861	1.50E-02	core barrel	"
	2-2227	299-E24-92	18.3	2	92	6	0	0	sand (2)	Hanford sand	0.1216	1.7364	0.0154	0.3271	8.70E-03	core barrel	"
	2-2228	299-E24-95	15.2	1	97	2	0	0	sand (2)	Hanford sand	0.8612	1.4523	0.0092	0.2925	2.10E-02	core barrel	"
	2-2229	299-E24-95	18.3	1	94	5	0	0	sand (2)	Hanford sand	0.1358	1.8345	0.0197	0.3070	6.40E-03	core barrel	"
	2-2230	299-E24-79	1.8	2	32	52	11	3	sand (2)	Hanford sand	0.0066	2.1407	0.0608	0.3309	2.30E-04	core barrel	"
	2-2231	299-E24-79	3.0	12	52	36	0	0	gravelly sand (4)	Hanford sand	0.0063	1.7824	0.0685	0.2811	7.50E-03	core barrel	"
	2-2232	299-E24-79	4.9	4	88	8	0	0	sand (2)	Hanford sand	0.0452	2.0873	0.0279	0.2450	4.10E-02	core barrel	"
	2-2233	299-E24-79	7.9	2	90	8	0	0	sand (2)	Hanford sand	0.3460	1.4491	0.0130	0.2906	1.70E-02	core barrel	"
	2-2234	299-E24-79	11.0	0	86	14	0	0	sand (2)	Hanford sand	0.0664	1.5548	0.0123	0.2782	2.10E-02	core barrel	"
US ECOLOGY [1,3]																	
MW-5	50	699-35-58	15.2	1	75	18	6	0	sand (2)	Hanford sand	0.0395	2.6308	0.0367	0.3309	3.53E-02	splitspoon	Bergeron et al., 1987
	70	699-35-58	21.3	0	38	51	11	0	sand (2)	Hanford sand	0.0142	4.7700	0.0300 [f]	0.4431	1.57E-03	splitspoon	"
	90	699-35-58	27.4	0	81	15	4	0	sand (2)	Hanford sand	0.0454	3.0831	0.0250	0.3854	2.26E-03	splitspoon	"
	130	699-35-58	39.6	0	28	68	4	0	sand (2)	Hanford sand	0.0150	4.9138	0.0250 [f]	0.4163	4.42E-02	splitspoon	"
	170	699-35-58	51.8	0	52	42	6	0	sand (2)	Hanford sand	0.0226	3.5355	0.0334	0.3927	3.81E-03	splitspoon	"
	190	699-35-58	57.9	1	84	11	4	0	sand (2)	Hanford sand	0.0473	2.8261	0.0200 [f]	0.4532	5.78E-03	splitspoon	"
	210	699-35-58	64.0	3	85	8	4	0	sand (2)	Hanford sand	0.0751	2.2980	0.0321	0.2724	5.42E-03	splitspoon	"
	230	699-35-58	70.1	0	77	18	5	0	sand (2)	Hanford sand	0.0393	3.1424	0.0100 [f]	0.4193	5.31E-03	splitspoon	"
	270	699-35-58	82.3	0	62	23	15	0	loamy sand (1)	Hanford sand	0.0244	1.5601	0.0200 [f]	0.3270	5.54E-04	splitspoon	"

	300	699-35-58	91.4	59	19	13	9	0	sandy gravel (5)	Middle Ringold	0.0105	1.6304	0.0123	0.1190	7.66E-04	splitspoon	"
MW-8	14.5	699-36-58B	4.4	0	78	18	4	0	sand (2)	Hanford sand	0.0425	3.1199	0.0395	0.4308	1.70E-03	splitspoon	"
	145	699-36-58B	44.2	0	2	58	40	0	sandy loam (1)	Hanford sand	0.0110	2.8937	0.0200 [f]	0.4233	8.86E-04	splitspoon	"
	185	699-36-58B	56.4	22	68	7	3	0	gravelly sand (4)	Hanford sand	0.0735	2.0899	0.0288	0.3074	7.19E-03	splitspoon	"
MW-10	45	699-36-58A	13.7	1	69	20	10	0	sand (2)	Hanford sand	0.0288	2.2830	0.0382	0.3385	5.31E-03	splitspoon	"
	86	699-36-58A	26.2	0	55	38	7	0	sand (2)	Hanford sand	0.0355	2.0852	0.0314	0.3822	1.97E-02	splitspoon	"
	105	699-36-58A	32.0	1	62	24	13	0	loamy sand (1)	Hanford sand	0.0233	1.9835	0.0408	0.3267	1.73E-02	splitspoon	"
	125	699-36-58A	38.1	1	59	30	10	0	sand (2)	Hanford sand	0.0210	2.8388	0.0429	0.3638	4.39E-03	splitspoon	"
	165	699-36-58A	50.3	1	59	30	10	0	sand (2)	Hanford sand	0.0186	3.4294	0.0373	0.3233	6.63E-03	splitspoon	"
	195	699-36-58A	59.4	24	57	13	6	0	gravelly sand (4)	Hanford sand	0.0312	2.0934	0.0298	0.2621	2.65E-03	splitspoon	"
	205	699-36-58A	62.5	10	71	12	7	0	gravelly sand (4)	Hanford sand	0.0503	1.7946	0.0258	0.2969	6.63E-03	splitspoon	"
	245	699-36-58A	74.7	0	71	20	9	0	sand (2)	Hanford sand	0.0319	2.3729	0.0321	0.3686	7.39E-03	splitspoon	"
	265	699-36-58A	80.8	0	64	25	11	0	sand (1)	Hanford sand	0.0259	2.5903	0.0160 [f]	0.3589	2.65E-03	splitspoon	"
	285	699-36-58A	86.9	0	64	26	10	0	sand (2)	Hanford sand	0.0282	2.6922	0.0170 [f]	0.3648	3.54E-03	splitspoon	"
	300	699-36-58A	91.4	0	71	22	7	0	sand (2)	Hanford sand	0.0291	3.1582	0.0281	0.3668	4.42E-03	splitspoon	"
VOC [2,4]	3-0647 [x]	299-W18-246	42.9	0	2	78	14	6	loamy sand (1)	Plio-Pleistocene	0.0051	2.0531	0.0400 [f]	0.4995	2.00E-04	splitspoon	Relyea, 1995
	3-0648	299-W18-246	59.6	62	18	20	0	0	sandy gravel (5)	Middle Ringold	0.0124	1.6450	0.0000	0.1462	8.70E-03	splitspoon	
	3-0649	299-W18-247	41.1	0	10	38	40	12	loam (1)	Plio-Pleistocene	0.0010	1.7024	0.0600 [f]	0.5331	N/A	splitspoon	"
	3-0650	299-W18-247	45.1	0	46	28	15	11	sandy loam (1)	Plio-Pleistocene	0.0120	1.5539	0.2412	0.6306	2.60E-07	splitspoon	"
	3-0651	299-W18-247	46.9	0	58	24	9	9	loamy sand (1)	Plio-Pleistocene	0.0286	1.9721	0.1006	0.3728	9.40E-03	splitspoon	"
	3-0652	299-W18-248	38.4	0	40	52	4	4	sand (2)	Hanford Sand	0.0092	1.8848	0.0300 [f]	0.3586	3.70E-04	splitspoon	"
	3-0653	299-W18-248	42.5	0	24	54	14	8	loamy sand (1)	Plio-Pleistocene	0.0067	1.8378	0.1096	0.4223	5.80E-06	splitspoon	"
	3-0654	299-W15-216	35.6	59	30	3	4	4	sandy gravel (5)	Plio-Pleistocene	0.0119	1.2618	0.0186	0.1933	2.70E-04	splitspoon	"
	3-0655	299-W15-216	36.9	34	28	8	24	6	silty sandy gravel (3)	Upper Ringold	0.0029	1.6285	0.0559	0.2625	1.58E-04	splitspoon	"
	3-0656	299-W15-216	39.0	42	40	18	0	0	sandy gravel (5)	Middle Ringold	0.0166	1.3941	0.0090	0.1814	1.36E-02	splitspoon	"
	3-0657	299-W15-217	37.4	34	38	10	10	8	silty sandy gravel (3)	Hanford Sand	0.0145	1.3692	0.0469	0.2505	2.67E-04	splitspoon	"
W-049-H [2,4]	2-2865 [x]	699-42-37	38.7	0	22	58	14	6	loamy sand (1)	Lower Ringold	0.0038	2.0069	0.1612	0.5868	2.30E-06	splitspoon	Delaney, 1992
	2-3084	699-41-39	24.7	82	14	4	0	0	sandy gravel (6)	Upper Ringold	0.0097	1.5700	0.0125	0.0579	1.30E-01	splitspoon	
	2-3085 [x]	699-41-35	31.5	0	55	25	10	10	sandy loam (1)	Lower Ringold	0.0142	1.2598	0.2705	0.6772	1.40E-08	splitspoon	"

	2-3088	699-42-37	4.6	65	20	12	3	0	sandy gravel (6)	Hanford Gravels	0.0038	1.5977	0.0197	0.1071	1.30E-03	splitspoon	"
	2-3089 [x]	699-42-37	28.3	0	35	30	27	8	sandy loam (1)	Hanford sand	0.0035	1.3657	0.1808	0.5336	3.20E-07	splitspoon	"
	3-0001	699-40-36	29.3	68	19	6	7	0	sandy gravel (5)	Hanford Gravels	0.0095	1.5556	0.0156	0.1128	1.82E-04	splitspoon	"
	3-0003	699-40-36	65.8	65	21	14	0	0	sandy gravel (5)	Basal Ringold	0.0054	1.4011	0.0538	0.1953	6.30E-07	splitspoon	"

[f] signifies that the residual moisture content has been fixed to improve the curve fit through the measured data

[#] soil category :

(1) - SS, sand mixed with finer fraction

(2) - S, sand

(3) - SSG, sand and gravel mixed with finer fraction

(4) - GS, gravelly sand

(5) - SG1, sandy gravel with gravel content approximately <60%

(6) - SG2, sandy gravel with gravel content approximately >60%

[x] sample containing swelling clay

1 - K_S measured by falling head permeameter

2 - K_S measured by constant head permeameter

Moisture Retention Data Measurements

3 - 0 to -60 cm, hanging water column; -100 to -15300 cm, pressure plate extraction (Klute 1986)

4 - 0 to -1000 cm, Tempe cell; -500 to -15300 cm, pressure plate extraction

5 - 0 to -150 cm, hanging water column; -310 to -15300 cm, pressure plate extraction; <-15300 cm, thermocouple psychrometer (Rawlins and Campbell 1986)

6 - 0 to -1000 cm, Tempe cell; -500 to -10000 cm, pressure plate extraction; < -10000 cm, thermocouple psychrometer

APPENDIX B: CODE LISTING FOR IMPLEMENTATION OF NEW PARAMETER DISTRIBUTIONS INTO LHS

```
c  program contlin.f
c-------------------------------------------------------------------------
c  This program generates a user-defined continuous distribution for Sandia's
c  Latin Hypercube Sampling (LHS) software.  The user inputs the mean,
c  standard deviation, and limits A and B (A < X < B) of a distribution that
c  has been transformed into a normal distribution.  Currently, the log ratio
c  and hyperbolic arcsine transformations as reported in Khaleel and Freeman
c  (1995) have been implemented in this code.  The output consists of an
c  LHS-readable file for a continuous linear distribution (p. 46, LHS User's
c  Guide, Wyss and Jorgensen).
c
c  Pseudo-code:
c  1) Have user enter in mean, standard deviation, and limits A & B of normal
c     distribution. Calculate values of A & B in real space using log ratio
c     or hyperbolic arcsine transformation.
c  2) Increment through standard normal variables starting with z=-3.4 (phi(z)
c     =0.0003 and ending with z=3.4 (phi(z)=0.9998).
c  3) Calculate quantile (cdf or phi(z)) for each z using approximation to
c     integral given in Handbook of Mathematical Functions, p. 932.
c  4) Transform standardized z to Y using Y=z*(s.d.) + mean.
c  5) Transform Y to a real-space variable X using either the log ratio or
c     hyperbolic arcsine transformation.
c  6) Increment z by a fixed amount and repeat (3) through (5).
c  7) If the change in X is more than 1% of the range given by limits A & B
c     (transformed into real space), then reduce z-increment by half and
c     repeat (3) through (5) and (7).
c  8) Output X and corresponding cdf (quantile) for the standardized variable,
c     z, corresponding to that X value.
c
c  C.K.Ho
c  9/10/98
c-------------------------------------------------------------------------
c234567890123456789012345678901234567890123456789012345678901234567890123456789012

      implicit double precision (a-h,o-z)
      real z(999),Y(999),X(999),phi(999),mu
      character*16 name
      character*19 out

      write(*,*)'This program will create a continuous linear'
      write(*,*)'distribution for LHS sampling.'
      write(*,*)
      write(*,*)'What is the variable name? (16 characters max)'
      read(*,*) name
      kend=index(name,' ')
      out=name(1:kend-1)//'.out'
      write(*,*)'What transformation has been used to obtain a normal'
      write(*,*)'distribution?'
      write(*,*)'1) log ratio'
      write(*,*)'2) hyperbolic arcsine'
      read(*,*) itrans
      write(*,*)'Enter mean of the untransformed distribution'
      read(*,*) rmu
```

```
      write(*,*)'Enter mean of the transformed (normal) distribution'
      read(*,*) mu
      write(*,*)'Enter s.d. of the transformed (normal) distribution'
      read(*,*) sig
      write(*,*)'Enter lower limit of untransformed distribution'
      read(*,*) A
      write(*,*)'Enter upper limit of untransformed distribution'
      read(*,*) B
      write(*,*)'The output for LHS-sampling will be in *.out'

      open(11,file=out,status='unknown')

c...Data
      step=0.2

c...Increment through standardized variable z starting at z=-3.4 and
c...ending at z=3.4
      i=1
      z(i)=-3.4

8     call cdf(i,z,phi)

      write(*,*) z(i),phi(i),B-A,change

c...Back-transform standardized variable z to Y

      Y(i)=z(i)*sig+mu

c...Transform Y to real space with log ratio or hyperbolic arcsine
c...transformation

      if(itrans.eq.1) then
        X(i)=(B*exp(Y(i))+A)/(1+exp(Y(i)))
      elseif(itrans.eq.2) then
        X(i)=(B-A)*sinh(Y(i))+A
      end if

c...Adaptive stepping:
c...Determine if change in X(i) from X(i-1) is less than 1% of the
c...range given by A and B.  If not, cut step size of z in half and
c...re-calculate cdf and subsequent transforms.
      if(i.gt.1) then
        change=(X(i)-X(i-1))/(B-A)
        if(change.gt.0.01) then
          step2=(z(i)-z(i-1))/2.
          z(i)=z(i-1)+step2
          go to 8
        end if
      end if

c...Increment i by 1 and increment z(i) by step.  Calculate new cdf
c...and subsequent transforms.
      i=i+1
      z(i)=z(i-1)+step

      if(z(i).le.3.4) goto 8

      nvar=i-1

c...Write output to LHS file
      write(11,20) name,rmu,nvar
20    format(a16,2x,e12.5,2x,'CONTINUOUS LINEAR',i5,' #')
      do i=1,nvar
```

```
        if(i.eq.1) then
          write(11,35) x(i),0.0,phi(i)
        elseif(i.gt.1.and.i.lt.nvar) then
          write(11,30) X(i),phi(i)
        elseif(i.eq.nvar) then
          write(11,35) x(i),1.0,phi(i)
        end if
      end do
30    format(e12.5,2x,e12.5,2x,'#')
35    format(e12.5,2x,e12.5,2x,'#',' $ Actual CDF= ',e12.5)

      stop
      end


c_____________________________________________________________________
      subroutine cdf(i,z,phi)

c   This subroutine calculates the cdf or quantile of the standardized
c   variable z.  The cdf is denoted as ph.
c_____________________________________________________________________

      implicit double precision (a-h,o-z)
      real z(999),phi(999)

c...Data
      p=0.2316419
      b1=.319381530
      b2=-.356563782
      b3=1.781477937
      b4=-1.821255978
      b5=1.330274429
      pi=4.d0*datan(1.d0)

c...Calculate cumulative distribution function (cdf) for standardized
c...variable z(i) using approximation in Handbook of Mathematical
c...Functions, Abramowitz and Stegun, 1964, 10th printing (1972),
c...p. 932, eq. 26.2.17, error < 7.5e-8

c...Because z must be greater than or equal to zero in the
c...approximation, use the absolute value in the formula, but
c...return 1-ph as the appropriate cdf if z is negative.

      zz=abs(z(i))

      t=1.d0/(1.d0+p*zz)
      pdf=dexp(-(zz**2)/2.d0)/dsqrt(2*pi)

      phi(i)=1-pdf*(b1*t+b2*t**2+b3*t**3+b4*t**4+b5*t**5)

      if(z(i).lt.0.d0) phi(i)=1-phi(i)

      return
      end
```

APPENDIX C: CODE LISTING FOR LINEAR RANK REGRESSION OF HYDROLOGIC PARAMETERS

```
C program rankreg.f
c_____________________________________________________________________
c  This program reads in columns of data and ranks the values in each
c  column.  A linear regression is then performed on the ranked values
c  for each pair of columns.  The correlation coefficient is determined
c  for each regression, and the original values, the ranked values, and the
c  correlation coefficients are printed.
c
c  xx(i,j)=original values for parameter i, sample j
c  nrx(i,j)=ranked values for parameteri, sample j
c  rx(j)=temporary sorting variable on j for paramter i
c  r(i,ii)=correlation coefficient for column i and column ii
c  b1, b0 = slope and y-intercept of linear regression fit
c  ncol=number of columns (parameters)
c  nrow=number of rows (samples)
c  nsumx=sum of the "x" values
c  nsumx2=sum of square of "x" values
c  nsumy=sum of the "y" values
c  nsumy2=sum of square of "y" values
c  nsumxy=sum of cross-products of each pair of parameters
c
c  C.K.Ho
c  9/1/98
c_____________________________________________________________________
c234567890123456789012345678901234567890123456789012345678901234567890123456789012
      implicit double precision (a-h,o-z)
      dimension xx(15,999),nrx(15,999),r(15,15),nsumxy(15,15),rx(999)
      dimension nsumx(15),nsumx2(15)
      dimension b1(15,15),b0(15,15)
      character*40 input,out1,out2,out3,prefix
      character*80 head

      write(*,*)'What is the name of the text file containing columns'
      write(*,*)'of data to be ranked and regressed?'
      read(*,*) input
      write(*,*)'Is there a header line in that file? (1=yes, 0=no)'
      read(*,*) nhead
      write(*,*)'How many columns of data are there?'
      read(*,*) ncol
      write(*,*)'What is the prefix of the desired output files?'
      read(*,*) prefix
      kend=index(prefix,' ')

      out1=prefix(1:kend-1)//'_R.txt'
      out2=prefix(1:kend-1)//'_orig.txt'
      out3=prefix(1:kend-1)//'_rank.txt'

      open(10,file=input,status='old')
      open(11,file=out1,status='unknown')
      open(12,file=out2,status='unknown')
      open(13,file=out3,status='unknown')

c...Read input file
      if(nhead.eq.1) read(10,'(a80)') head
```

```
      j=1
11    read(10,*,end=99) (xx(i,j),i=1,ncol)
      j=j+1
      go to 11
99    nrow=j-1

      write(*,20) ncol,nrow
20    format('Have read in',i5,' parameters and ',i5,
     &       ' samples...')


c...Rank each parameter in each column using a multipass sorting routine
c...Sort variables rx(j); then assign the rank, nrx(i,j) according to
c...the index j in rx(j) by matching xx(i,j) with rx(j)
c234567890123456789012345678901234567890123456789012345678901234567890123456789012
      nsort=1
      do i=1,ncol
c...Assign  rx(j)=xx(i,j) for sorting purposes
        do j=1,nrow
          rx(j)=xx(i,j)
        end do
33      if(nsort.eq.1) then
          nsort=0
          do j=1,nrow-1
            if(rx(j).gt.rx(j+1)) then
              temprx=rx(j)
              rx(j)=rx(j+1)
              rx(j+1)=temprx
              nsort=1
            end if
          end do
          go to 33
        end if

c        write(*,*) (rx(j),j=1,nrow)

c...rx(j) is now sorted for parameter i.  Assign a rank, nrx(i,j) for
c...each parameter xx(i,j) based on the index k in rx(k)
        do j=1,nrow
          do k=1,nrow
            if(xx(i,j).eq.rx(k)) then
              nrx(i,j)=k
              go to 37
            end if
          end do
37      end do
        nsort=1
        write(*,40) i
40      format('Have ranked parameter ',i5,'...')
      end do

c...Perform a linear regression analysis on each parameter (column) pair

c...Find sum of columns and cross-products for each pair of parameters
c   nsumxy(i,ii)=sum of products of x times y for columns i and ii

c...First initialize all nsum to zero.
      do i=1,ncol
        nsumx(i)=0
        nsumx2(i)=0
        do ii=1,ncol
          nsumxy(i,ii)=0
        end do
```

```
      end do

c...Calculate sum of entries in each column, x(i) and y(i), and the sum of
c...the squares of the entries in each column
c...nsumx(i)=sum of all "x" values in column i
c...nsumx2(i)=sum of square of "x" values in column i
      do i=1,ncol
        do j=1,nrow
          nsumx(i)=nsumx(i)+nrx(i,j)
          nsumx2(i)=nsumx2(i)+nrx(i,j)*nrx(i,j)
        end do
c        write(*,13) nsumx(i),nsumx2(i),i
c13      format('nsumx(i)= ',i3,'; nsumx2(i)= ',i3,'; i= ',i2)
      end do


c...Calculate sum of cross-products for all possible pairs of columns of
c...data (top half of symmetric matrix only)
      do i=1,ncol
        do ii=1,ncol
          do j=1,nrow
            nsumxy(i,ii)=nsumxy(i,ii)+nrx(i,j)*nrx(ii,j)
          end do
c          write(*,17) nsumxy(i,ii),i,ii
c17        format('nsumxy= ',i3,'; i= ',i2,' ii= ',i2)
        end do
      end do

c...Determine coefficients for linear regression (b1=slope, b0=y-intercept)
c...and correlation coefficient, r, for
c...all pairs of columns of data (Probability and Statistics for
c...Engineering and the Sciences, J.L. Devore, 1982, Brooks/Cole
c...Publishing Co., Monterey, CA, p. 429, p. 448)
c...Note that for a rank regression the slope is equal to the correlation
c...coefficient.
c234567890123456789012345678901234567890123456789012345678901234567890123456789012
      do i=1,ncol
        do ii=1,ncol
          b1(i,ii)=(nrow*nsumxy(i,ii)-nsumx(i)*nsumx(ii))/
     &      (nrow*nsumx2(i)-nsumx(i)**2.d0)
          b0(i,ii)=(nsumx(ii)-b1(i,ii)*nsumx(i))/nrow
          r(i,ii)=(nrow*nsumxy(i,ii)-nsumx(i)*nsumx(ii))/
     &      (dsqrt(nrow*nsumx2(i)-nsumx(i)**2.d0)*dsqrt(nrow*nsumx2(ii)-
     &      nsumx(ii)**2.d0))
c          write(*,18) b1(i,ii),i,ii
c          write(*,19) b0(i,ii),i,ii
c          write(*,17) nsumxy(i,ii),i,ii
c          write(*,23) nsumx**2,i,ii
c23        format('nsumx**2 ',i4,'; i= ',i2,' ii= ',i2)
c18        format('b1(i,ii)= ',e10.4,'; i= ',i2,' ii= ',i2)
c19        format('b0(i,ii)= ',e10.4,'; i= ',i2,' ii= ',i2)
        end do
      end do

c...Fill out the rest of the symmetric matrix
c      do i=2,ncol
c        do ii=1,i-1
c          b1(i,ii)=b1(ii,i)
c          b0(i,ii)=b0(ii,i)
c          r(i,ii)=r(ii,i)
c        end do
c      end do
```

```
c...Write output to files
      write(12,*)'Actual Values'
      write(13,*)'Ranked Values'
      if(nhead.eq.1) then
        write(11,'(a)') head
        write(12,'(a)') head
        write(13,'(a)') head
      end if
      do j=1,nrow
        write(12,75) (xx(i,j),i=1,ncol)
        write(13,77) (nrx(i,j),i=1,ncol)
      end do
75    format(15(e12.5,2x))
77    format(15(i4,2x))

      write(11,*) 'correlation coefficient (r)'
      do i=1,ncol
        write(11,75) (r(i,ii),ii=1,ncol)
      end do

      write(11,*)

      write(11,*) 'slope (b1)'
      do i=1,ncol
        write(11,75) (b1(i,ii),ii=1,ncol)
      end do

      write(11,*)
      write(11,*) 'y-intercept (b0)'
      do i=1,ncol
        write(11,75) (b0(i,ii),ii=1,ncol)
      end do

      stop
      end
```

DISTRIBUTION

1 David L. Becker
717 S. Jefferson Street
Kennewick, WA 99336-9364

1 Ed Fredenburg
Lockheed Martin Hanford Corporation
H7-07
P.O. Box 1500
Richland, WA 99352-1505

1 Phil Rogers
Jacobs Engineering Group
507 Knight Way, Suite B
Richland, WA 99352

1 Raz Khaleel
Fluor Daniel Northwest, Inc.
B7-50
P.O. Box 1050
Richland, WA 99352-1050

1 Aki Runchal
Analytic & Computational Research, Inc.
1931 Stradella Road
Bel Air, CA 90077

1 Gary Smith
Dept. of Earth and Planetary Sciences
University of New Mexico
Albuquerque, NM 87131

1 MS-0771 M. Chu, 6800
1 MS-0734 L. Bustard, 6803
1 MS-0748 L-J. Shyr, 6331
1 MS-0778 R. Baca, 6851
1 MS-0747 T. Wheeler, 6412
1 MS-1345 S. Conrad, 6416
1 MS-0701 L. Shephard, 6100
1 MS-0735 P. Davies, 6115
10 MS-0735 C. Ho, 6115

1 MS-9018 Central Technical Files, 8940-2
2 MS-0899 Technical Library, 4916
1 MS-0619 Review & Approval Desk, 15102
For DOE/OSTI